Draining a Tank

an appendix to

Dimensional Analysis of Models and Data Sets

James F. Price
Dept. of Physical Oceanography, Woods Hole Oceanographic Institution
Woods Hole, Massachusetts, 02543
http://www.whoi.edu/science/PO/people/jprice · jprice@whoi.edu

January 14, 2026

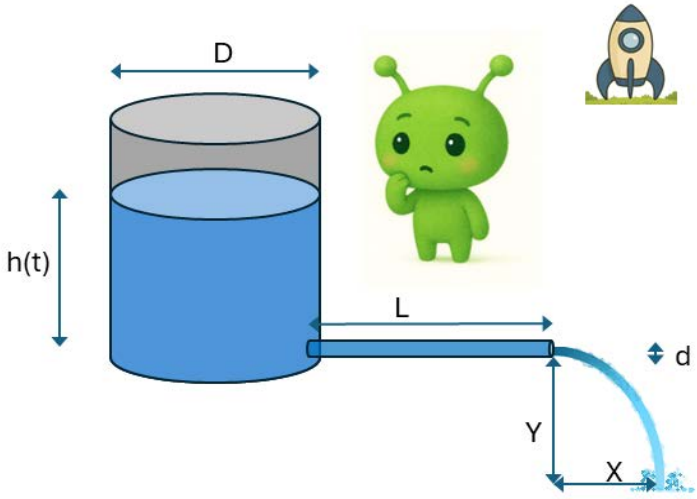

Planetary Explorer contemplating a water tank.
By the author using ChatGPT-5.

How long to drain this tank?

Here to learn Earth's ways.
All I see are water tanks —
deeper than they seem?

Summary

We can help. The objectives of this appendix are to observe and then model the time it takes a gravity-driven outflow to drain a tank. The observations come from a family of experiments that explore the effects of two real-fluid properties of water, surface tension and viscosity. Surface tension may slow the outflow as the fluid height becomes small, and in some cases stop it altogether. When a pipe is present, viscous drag will reduce the outflow by a factor that depends upon the fluid viscosity, the diameter and length of the pipe, d and L, and the height of the surface, h.

The goal of this appendix is to demonstrate dimensional analysis as a guide for organizing this multi-parameter dataset into a concise and interpretable form. A clear organization of the data facilitates comparison with model predictions and highlights specific errors. This leads to a sequence of improved models. The end result is a model that is mostly understandable while providing reliable solutions for the parameter space of the present experiments.

Contents

1 Draining a tank; objectives and goal

"How long to drain this tank?" comes up in a wide range of contexts. Tank-draining projects are a mainstay of physics education, where they combine accessible experiments with satisfying theory.[1] Tank-draining problems continue to be a research topic in nuclear and chemical engineering when they include complex plumbing and highly exotic fluids.[2]

Though simple in concept, tank-draining problems do not admit simple solutions except in the most idealized case in which the fluid is considered to be ideal. This study goes beyond the basic case by including two real-fluid properties of water, surface tension and viscosity. Modeling these phenomena, the objective of this appendix, requires experimental observations and theory combined in roughly equal measure. The deeper goal of this appendix is to show how dimensional analysis can be the essential link between observations and a theory.

Readers are assumed to have some experience with applied mathematics including linear algebra and ordinary differential equations, and classical mechanics to include a first look at fluid mechanics. This article is meant to be suitable for self-study.

1.1 Why and how dimensional analysis

The procedure of dimensional analysis followed here is outlined briefly below and in considerably greater detail in the main text, Dimensional Analysis of Models and Data Sets.[3] If dimensional analysis strikes you as abstract in the extreme — as it does for *everyone* who is new to the idea — then Secs. 1 - 3 of the main text are strongly recommended as a prerequisite to this appendix. If you are somewhat familiar with dimensional analysis as it is usually practiced via the Buckingham Pi Theorem, then you will find that the present method is different mainly by the approach to 3) and 4) below.

1. **Problem definition.** A problem is defined by a so-called Variables and Parameters list, or VPlist, that starts with one dependent variable, the unknown, and includes all of the other variables and parameters that would necessarily appear in a model of the phenomenon. A

[1] Donnelly, S. C., et al., 2024, Draining a tank through multiple orifices: An improved lab experiment in fluid mechanics, https://doi.org/10.18260/1-2-660-46367, and Rother, M. A., 2024, Modelling tank drainage using a simple apparatus. Journal of Mathematical Education in Science and Technology. 55, 2, 295 - 307. https://doi.org/10.1080/0020739X.2023.2249472 .

[2] Elgamal, M., K. Kriaa and M. Farouk, 2021, Drainage of a Water Tank with Pipe Outlet Loaded by a Passive Rotor. Water, 2021, 13, 872 https://doi.org/10.3390/w13131872

[3] Online at https://ocw.mit.edu/courses/res-12-001-topics-in-fluid-dynamics-fall-2024/

remarkable property of dimensional analysis is that you do not have to know the model in any further detail; though better of course, if you do. These variables and parameters are characterized by the powers (the exponents) on their fundamental dimensions, [mass length time]. For example, the dimensions of a pipe having length, L, will be indicated by a dot-equals notation, e.g., $L \doteq [0\ 1\ 0]$, a speed $V = dL\,/\,dt$ has dimensions $V \doteq [0\ 1\ -1]$, and an acceleration has dimensions $dV/dt \doteq [0\ 1\ -2]$. The powers of each member of the VPlist (the three-element row vectors above) are collected into a dimension matrix.

2. **The practical advantages of dimensional analysis.** If the VPlist is complete, then the dependent variable may be written in a nondimensional form that is free from reference to a system of units, e.g., meters, centimeters or feet, and so is a pure number. There are two significant advantages in this that will be highlighted as we go through this analysis. First, a description in nondimensional variables is more concise (has fewer variables) than is the equivalent dimensional description. Second, a nondimensional description helps focus attention on meaningful relationships. For example, a pipe may be judged to be long or short compared to the pipe diameter, a natural scale with physical significance, or in meters or centimeters, arbitrary scales. The latter system is likely to be most useful during the design and execution of an experiment, while the use of nondimensional variables will maximize the utility of the experimental results.

3. **Automated calculation of nondimensional variables.** The nondimensional variables may be computed by solving a system of linear equations for the null space of the dimension matrix. The solution vectors of the null space correspond one-to-one with nondimensional variables. This calculation is not difficult, but can be tedious if done by hand. The calculation is quick and sure when automated; links to Matlab and Python codes are in Sec. 8.

4. **Interpretation.** The system of equations is most often undetermined, i.e., more unknowns than independent equations. In that case the initial basis set is not unique, and it will be optimal only by chance. Your task will be to transform (as necessary) the initial basis set into a form that will enhance the utility and interpretation of the analysis. Examples of this transformation will be seen throughout.

Planetary Explorer beginning a long trek.
Image by the author using ChatGPT-5.

Seeking a better model.

A long path ahead.
Starlit by the Milky Way,
I'll take slow, sure steps.

1.2 Model development guided by observations and dimensional analysis

The model development described here takes place in five steps, Fig. 1, each one motivated by a comparison of model predictions with a suite of experimental observations. Dimensional analysis is a great help in organizing the observations, and so guiding the next step in the model development.

There are two ideals for the model — sufficient transparency that we can understand what the model is and what it does, and, that the model predictions be true to the observations. These are not easily achieved at once. In the progression of models shown in Fig. 1, Model 4 is transparent and understandable but makes a consistent overestimate of the outflow transport. Model 5 utilizes historical, empirical turbulent pipe flow correlations to modify the viscous drag calculated by Model 4. This largely corrects the overestimation errors, but with some loss of transparency. The intent here is to be deliberate and clear about these tradeoffs.

Sec. 2. The next section describes the experiments and the resulting data that are essential to this study. The present family of experiments is defined by a four-dimensional parameter space — orifice or pipe diameter, pipe length, fluid height, and fluid viscosity. The aim of this study is not to answer any one specific tank-draining problem, helpful as that might be, but rather to model and understand the entire family of experiments defined by the available apparatus.

Sec. 3. The first experiments are made without a pipe, or orifice-only. The observed surface height, $h(t)$ is almost parabolic in time, and is described well by the most elementary model, Model 1, until h becomes very small. The observed outflow then slows and may stop altogether before the tank

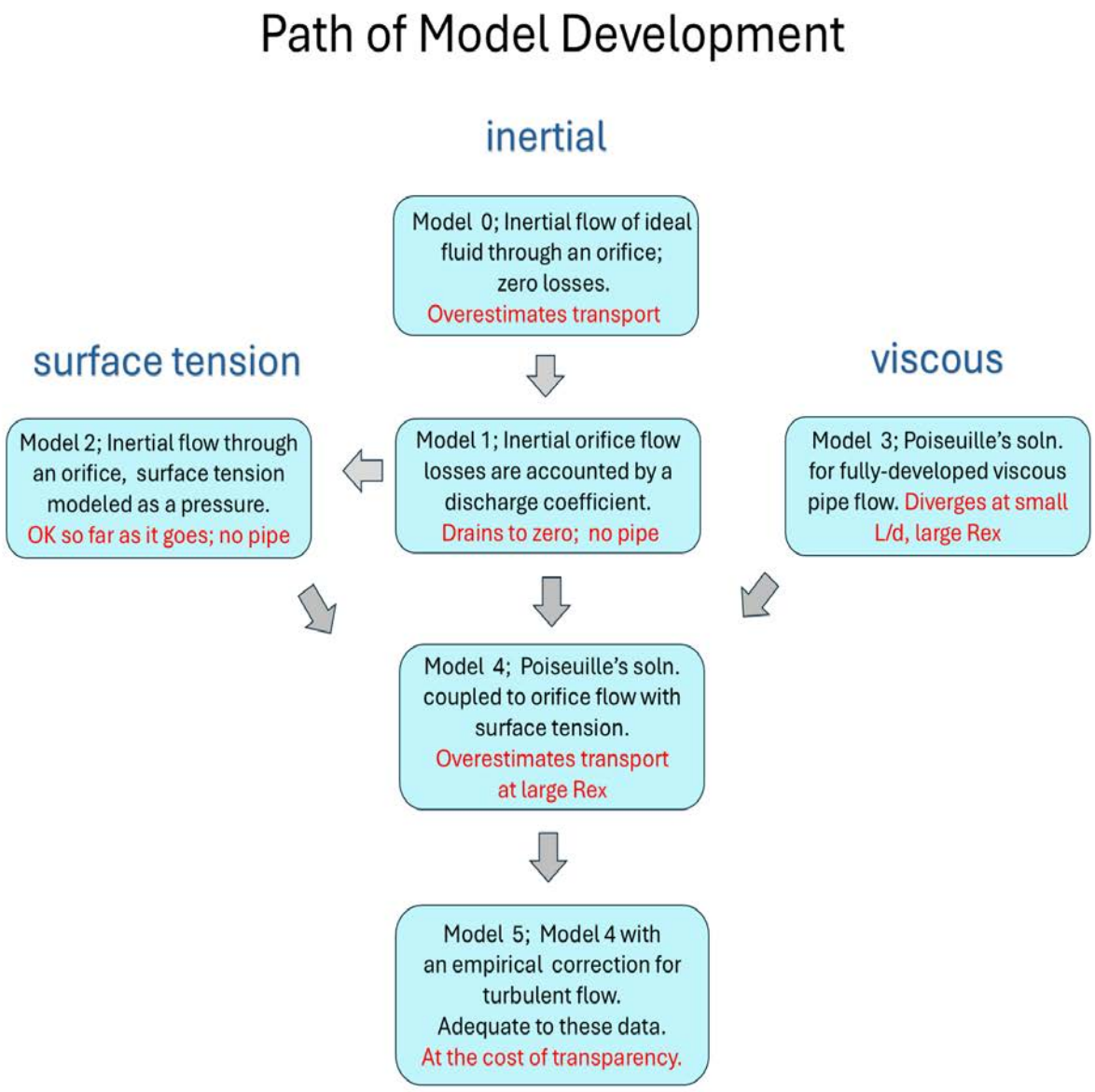

Figure 1: The sequence of models developed here, starting from very simple at the top to fairly complex at the bottom. A narrative of this model progression is in Sec. 1.2. There are at first two tracks that treat two distinct physical properties of real water. The track at left deals with surface tension, and the track at right deals with viscous effects. Surface tension and viscosity are treated separately until brought together in Model 4. The final Model 5 implements an empirical correction for the greater wall stress that occurs at larger Reynolds number consistent with the occurrence of turbulent flow. The red text in a box notes a salient shortcoming.

drains completely. In some respects this is a small detail, but it is also a qualitative error that is inherent to the ideal fluid model implicit in Model 1. How can we improve on this?

Sec. 4. At small values of h the orifice may be blocked by a stationary bubble or cap of fluid. From appearance alone this suggests an effect of surface tension, treated briefly in Sec. 4, and implemented as Model 2.

Sec. 5. The emphasis of this study is on the viscous drag that accompanies outflow through a pipe. Dimensional analysis is used to organize observations in a way that reveals the systematic and large amplitude variation of the outflow transport with pipe length, pipe diameter, viscosity and surface height. This empirical relationship is the objective of later Models 4 and 5.

Sec. 6.1 Poiseuille's historically significant and still quite useful model of fully-developed, viscous, laminar pipe flow is taken as Model 3. It shows promise for cases with longer pipes and greater viscous drag. However, it diverges toward unrealistic, excessive transport for cases with lesser drag because it takes no account of the inertial acceleration that has to accompany the movement of fluid from the tank into and through the orifice.

Sec. 6.2 A hybrid Model 4 combines Poiseuille's solution with the inertial orifice flow of Model 1 and surface tension of Model 2. A surprising result is that the solution of Model 4 can be written as a function of one nondimensional independent variable where dimensional analysis had indicated two independent variables. The collapsed, one variable description leads to a more insightful diagnosis of the advective/diffusive balance within the laminar flow regime. Model 4 gives a reasonable, semiquantitative account of the observations overall, however it displays a systematic overestimate of transport (underestimates viscous drag) for cases with larger Reynolds numbers.

Sec. 7 The inference made from this observation is that the flow is turbulent at the larger Reynolds numbers reached in these experiments. Modeling turbulent flow relies on historical data correlations. The resulting Model 5 is adequate to these data, but at some cost in transparency, i.e., Model 5 is not understandable to the depth of Model 4.

1.3 Glossary of symbols, phrases and models

- **Symbols**
  - C orifice discharge coefficient; for this apparatus, $C \approx 0.77$, nondimensional
  - d inside diameter of the orifice and the pipe
  - D diameter of the cylindrical water tank
  - F is an unknown function
  - g acceleration of gravity, 9.8 m s^{-2} and presumed constant

- h height of the water surface above the orifice/pipe center
- Q observed volume transport of the outflow, m^3 s^{-1}
- μ dynamic viscosity, for water, nominal 0.9 $\times 10^{-3}$ Pa s, temperature dependent
- $\nu = \mu/\rho$ kinematic viscosity, for water, nominal 0.9 $\times 10^{-6}$ m^2 s^{-1}
- ν_e equivalent viscosity that mimics the enhanced wall stress of turbulent flow
- r radius of the orifice or pipe = $d/2$
- ρ the density of fresh water, 998 kg m^{-3} and presumed constant
- σ surface tension, for water, nominal 75×10^{-3} N m^{-1}, or 75×10^{-3} kg s^{-2}
- W volume of fluid in the tank, m^3
- $\doteq$ 'dot equals' is an operator that brings out the exponents on [mass, length, time], e.g., $W \doteq$ [0 3 0] and $Q = -dW/dt = \doteq$ [0 3 -1].

- **Derived Symbols and Phrases**
  - $a = \pi d^2 / 4$, area of the orifice and pipe
  - $A = \pi D^2 / 4$, area of the tank
  - $E = (L/d)\, Re_x^{-1} = (L\,\nu)/\, d^2 \sqrt{2\ g\ h}$
  - $h_\sigma = \sigma /(\rho\, g\, r)$, equivalent hydrostatic head of the surface tension-induced pressure
  - $V_a = Q\,/\,a$, area-averaged velocity of the outflow, known only if Q is known
  - $V_T = \sqrt{2\, g\, h}$, Torricelli velocity, considered external when h is a known, independent variable
  - $Re = V_a\, d\,/\nu$, the most commonly encountered version of a pipe Reynolds number
  - $Re_x = V_T\, d\,/\nu$, the external Reynolds number used frequently here
  - basis set of nondimensional variables, calculated by the codes linked in Sec. 8.
  - entry length, the distance downstream from the orifice over which the flow becomes independent of distance, also said to be fully-developed
  - hydrostatic head, the height of a fluid at rest that gives a specific pressure
  - laminar flow implies a steady, one-dimensional velocity throughout the pipe, and a simple relationship between frictional drag and transport
  - turbulent flow implies unsteady, three-dimensional, and dispersive velocity, with one consequence being greater drag than in an otherwise comparable laminar flow
  - VPlist, variables and parameters in a list that defines a problem.

- **Glossary of Models**

- Model 0, Q_0, a zero-order model of orifice transport, $Q_0 = a V_T$, Eq. (11)
- Q_1 the elementary model of orifice transport, $Q_1 = C Q_0$, Eq. (14)
- Q_2 as Q_1 including surface tension, $Q_2 = Q_1 \sqrt{1 - h_\sigma / h}$, Eq. (22)
- Q_3 Poiseuille's solution for viscous, laminar flow through a pipe, Eq. (35)
- Q_4 a solvable, hybrid model that includes Q_1, Q_2 and Q_3, Eq. (40)
- Q_4' Model 4, but with a prime indicating no surface tension, implicitly via Eq. (41)
- Q_5 as Q_4 with a correction for turbulent flow, Eq. (56)
- Q_5' as Q_5 but omits surface tension.

2 A family of experiments

This study is built around a dataset generated during a series of low-tech, tabletop experiments that can be readily reproduced and extended. The tank was a polypropylene, semi-transparent laboratory beaker into which holes of known diameter, orifices, were drilled carefully a few centimeters above the bottom. For most experiments, there was a polypropylene tube connected directly to the orifice (very much like the cover page illustration) and kept horizontal. The length of this 'pipe' could be easily cut down, including to effectively zero. The fluid was ordinary tap water, whose viscosity, μ, and surface tension, σ, are well-known functions of temperature.

2.1 Parameter space of this apparatus

The immediate aim of the experiments was to document the time to drain (or more generally the draining rate) over the accessible range of the independent parameters that define this family of experiments:

- orifice or pipe diameter, $3 \leq d \leq 6.5$ mm,
- pipe length, $0 \leq L \leq 1.5$ m,
- fluid viscosity, $0.6 \times 10^{-3} \leq \mu \leq 1.5 \times 10^{-3}$ Pa s, depending upon water temperature,
- surface height, $0 \leq h \leq 0.15$ m.

Other relevant parameters that were not varied in these experiments:

- $\sigma = 75 \times 10^{-3}$ N m^{-1}, surface tension of fresh water at room temperature,
- $D = 0.185$ m, the tank diameter,
- $g = 9.8$ m s^{-2}, acceleration of gravity, and

- $\rho = 998$ kg m^{-3}, the nominal density of fresh water.

This apparatus is intermediate in scale — it is much larger than the scales of biological, capillary flows, and it is much smaller than the scales of a continent-spanning natural gas pipeline. The resulting flows may be characterized as low speed, low energy, and mostly *laminar*. However, in the higher range of Reynolds numbers accessed here there are fairly clear signs of weakly *turbulent* flow discussed in Sec. 7.

2.2 Making observations

Experiments began by filling the beaker with water having a measured temperature ranging from very hot to almost freezing. Once the fluid had settled (observed with dye), the orifice or pipe was uncovered, and the water allowed to drain freely. The beaker had a volumetric scale, and the elapsed time was recorded as the surface descended by discrete intervals of volume, W_i = (4.5, 4.0, 3.5 ... 0.5) $\times$ 10^{-3} m^3, and thus the direct observation was of W_i at about 8 - 12 times, t_i. Most experiments were complete within twenty minutes. The surface height in meters referenced to the orifice center (where $W = W_0$) is easily calculated by

$$h_i = (W_i(t) - W_0)/A, \tag{1}$$

where $A = \pi D^2/4$ is the surface area of the tank. A closely related variable is the outflow volume transport, Q, estimated by first-differencing the discrete, observed volumes and times,

$$Q_i \approx -\frac{W_{i+1} - W_i}{t_{i+1} - t_i}. \tag{2}$$

The sign convention ensures that the estimated outflow $Q > 0$, to aid visualization. The h that goes along with (2) is the midpoint average $\bar{h_i} = (h_{i+1} + h_i)/2$, and similarly for the time. From here on the subscripts and accents are dropped, and h, t and Q are treated as if continuous.

The measurements were found to be nearly repeatable, with random errors in the time estimated to be no more than 2 seconds. These small errors do not accumulate during the course of an experiment, and may be suppressed by a three-point smoothing of the observed times (applied in only a few cases). The largest source of systematic error comes from defining the inside diameter of the tube, d. For each tube, the diameter was measured by feeler gauges and often found to be slightly different, by as much as 0.1 mm, from the diameter indicated by the manufacturer (not a problem for the orifice diameter, which is well-controlled). Uncertainty in d is magnified by the sensitive dependence upon d that characterizes several aspects of tank-draining, e.g., outflow transport $Q \propto d^2$. The net uncertainty on any one estimate of Q is roughly $\pm 10\%$ of the magnitude.

These measurements were neither highly resolved nor highly precise. That is less than ideal, of

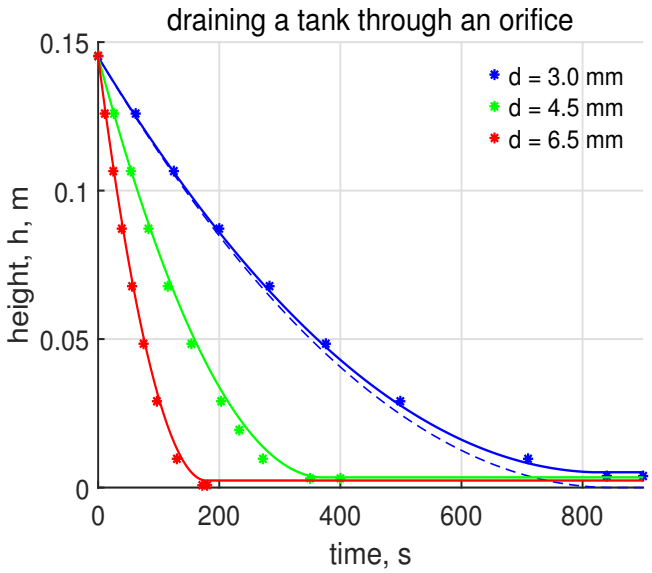

Figure 2: Surface height, $h(t)$, from three orifice-only experiments that had different orifice diameters, the red, green and blue dots. The trajectories $h(t)$ are very nearly parabolic, a rapid decrease at the beginning that markedly slows as h decreases. These experiments show that a modest increase in orifice diameter resulted in a substantially faster decrease of the surface height. Notice that the surface height stops descending short of zero. The dashed blue line is the ideal fluid Model 1 solution for the case $d = 3.0$ mm. Model 1 ignores surface tension and so this solution drains to zero. The solid lines are computed by Model 2 which acknowledges surface tension (coming in Sec. 4).

course, but it is not disqualifying because the case-to-case variation with changing parameters is considerably greater than are the random or systematic errors that compromise the value of any one realization. Thus, we can with some confidence explore and seek to model the parameter dependence of h and Q, over the family of experiments. Dimensional analysis is especially useful in this context.

2.3 Inferences from the first experiments

The first set of experiments used room temperature water, $T = 20\,^{\circ}C$, and no pipe (orifice-only) and so L was effectively zero. The orifice diameter was $d = 3, 4.5$ or 6.5 mm. The surface height $h(t)$, here regarded as the dependent variable, decreased smoothly in time, Fig. 2. Notice that the variation of h with d — the signal we are after — is considerably greater than are the likely experimental errors noted above.

After several trials with dimensional analysis, it became evident that the usual tank-draining problem — *How long to drain this tank?* — was best approached indirectly.

The first issue is that in some experiments the tank never actually drained in the strong sense $h \to 0$. At the beginning of an experiment, when h was largest, the outflow makes a continuous stream, or jet, of water that traces out what appears to be a ballistic trajectory. As h becomes small, less than a few centimeters, the outflow may slow significantly and then stop when h was still roughly 1 cm above the center of the orifice. The fluid then forms an outward protruding cap or bubble that is evidently held in place by surface tension and adhesion to the beaker. Surface dynamics of this kind is central to many small scale fluid problems and is discussed briefly in Sec. 4.

A second issue is that a response to the original problem (how long?) implies the construction of a model relationship for the time-dependent height, $h(t)$, and its dependence on the variables and parameters that define an experiment. Consider the simplest possible version of this: draining an ideal fluid (zero surface tension and zero viscosity) through an orifice (zero pipe length). In Sec. 3.1 below we will examine a very simple and effective model for this problem. But suppose we do not know the model — we can still make progress via dimensional analysis provided only that we can compile a list of the variables and parameters that would appear in an appropriate model.

- A VPlist for the surface height of an ideal fluid draining through an orifice:

1. surface height, $h \doteq [\,0 \quad 1 \quad 0\,]$, the dependent variable,
2. time, $t \doteq [\,0 \quad 0 \quad 1\,]$, an independent variable,
3. initial height, $h_0 \doteq [\,0 \quad 1 \quad 0\,]$, a parameter,
4. diameter of the orifice, $d \doteq [\,0 \quad 1 \quad 0\,]$, a parameter,
5. diameter of the tank, $D \doteq [\,0 \quad 1 \quad 0\,]$, a parameter,
6. acceleration of gravity, $g \doteq [\,0 \quad 1 \quad -2\,]$, a parameter.

If this list is indeed complete, then we can assert that there is, in principle, a relationship

$$h \;=\; F(t, h_0, d, D, g). \tag{3}$$

The function F is unknown, and it is, of course, crucial. Experimental data are required to show what F might be.

Now consider the nondimensional counterpart of (3). This VPlist has six members having two fundamental units, length and time. Our rule-of-thumb guidance to the number of required nondimensional variables (discussed in the main text, Sec. 3) indicates that a basis set for this VPlist (notice that it is not *the* basis set) will contain six minus two = four nondimensional variables. As one possibility, the nondimensional version of (3) could be

$$\frac{h}{h_0} \;=\; F(t\sqrt{g/h_0},\; \frac{d}{D}, \frac{h_0}{D}). \tag{4}$$

The Eq. (4) recycles the symbol F to represent an unknown function. The dependent variable is h in units that are natural to the problem, h_0.[4] Similarly, the orifice diameter d is in units of the tank diameter, D, and time is measured by the time required to free-fall a distance h_0 while accelerating at g. In place of five dimensional variables in the F of Eq. (3), there are just three nondimensional variables in the F of (4). That is a very useful, practical result from dimensional analysis.

[4]One could just as well say that h is measured by, divided by, scaled by, or nondimensionalized by h_0.

Dealing with three independent nondimensional variables is certainly possible (many real-life problems are far more extensive), and yet (4) seems unduly cumbersome given how straightforward and spare this problem appears to be. It will often happen that the first try at a VPlist will have a broader scope than is desirable for the problem at hand — in this case, slow outflow due mainly to the property that $d \ll D$. How can we change the problem and the VPlist to reflect that qualification?

2.4 Changing the problem

The surface height, h, is very important in what follows. Nevertheless, h may not be the best choice for the dependent variable. The reason, shown below, is that a model of $h(t)$ necessarily requires the time, t, and the tank diameter, D, as parameters.

Suppose instead that we seek a model of the volume transport, Q, of the outflowing water, Eq. (2). A key modeling assumption appropriate to this new problem is that Q depends only (or mainly) upon local conditions, and specifically the pressure difference across the orifice. As a corollary of this, the beaker diameter is large enough compared to the orifice that the beaker may be viewed as an infinite reservoir of water that is effectively at rest. D will then have a negligible effect upon the volume transport, though it will remain an essential parameter in any model that seeks to compute the time to drain, as in (4). Since $d << D$, the flow within the tank is very slow compared to the outflow velocity, and the acceleration of the water in the tank is negligible compared to g. The pressure $P(z)$ within the beaker is then given accurately by the hydrostatic pressure,

$$\frac{\partial P}{\partial z} = -\rho g, \tag{5}$$

and so

$$P(z) = \rho g (h - z) + P_{atm}, \tag{6}$$

where z is the vertical coordinate positive up and zero at the orifice, and ρ is the constant density of the fluid.[5] P_{atm} is the ambient, atmospheric pressure which varies insignificantly over the depth of the tank. The pressure difference across the orifice is, provisionally, just

$$\delta P_{orf} = \rho g h, \tag{7}$$

the hydrostatic pressure inside the tank at the depth of the orifice. The important variable of (7) is h; g and ρ are necessary to have the units of pressure, but are global constants in this family of experiments.

[5]To here this is the usual, elementary tank-draining problem. An advanced treatment is by D'Alessio, S., 2021, Torricelli's law revisited. European J. of Physics, 42 065808.

- A VPlist for the pressure-driven volume outflow of an ideal fluid through an orifice:

1. outflow volume transport, $Q \doteq$ [0 3 -1], the dependent variable,
2. surface height above the orifice, $h \doteq$ [0 1 0], the independent variable,
3. diameter of the orifice, $d \doteq$ [0 1 0], a parameter,
4. acceleration of gravity, $g \doteq$ [0 1 -2], a parameter,
5. density of the fluid, $\rho \doteq$ [1 -3 0], a parameter.

A quick calculation of a null space basis from this VPlist leads to

$$\frac{Q}{d^2\sqrt{g\,h}} \;=\; F(\frac{h}{d}), \tag{8}$$

which has only one independent, nondimensional variable: this represents major progress from Eq. (4).

2.5 Problems

- In Sec. 2.4 the tank-draining problem was changed from modeling $h(t)$ to modeling $Q(h)$. How and why did this change the status of the variable h?
- What dimensional variables or parameters have gone missing from Eq. (8) compared with Eq. (4), and on what basis?

3 An elementary (and very successful) Model 1

3.1 Torricelli velocity and a zero-order model

Eq. (8) could be used as is, but it is helpful to modify it superficially by introducing two O(1) numerical factors,

$$\frac{Q}{\frac{\pi}{4}d^2\sqrt{2\,g\,h}} \;=\; F(\frac{h}{d}). \tag{9}$$

A factor $\pi/4$ multiplies d^2 to give the area of the orifice,

$$a \;=\; \frac{\pi}{4}\,d^2.$$

A factor $\sqrt{2}$ multiplies $\sqrt{g\,h}$. The latter follows from the conservation of energy of a particle falling a distance h under gravity and acquiring kinetic energy $\propto\; V^2/2 \;=\; g\,h$. The velocity of an

energy-conserving free fall is then

$$\boxed{V_T \;=\; \sqrt{2\,g\,h}} \tag{10}$$

dubbed the Torricelli velocity.[6]

The product of V_T and the area of the orifice makes a sensible, physically-based natural scale for the outflow transport,

$$\boxed{Q_0 \;=\; a\,V_T \;=\; a\,\sqrt{2\,g\,h}} \tag{11}$$

In the main text this sort of thing was called a zero-order model, here shortened to Model 0 and for the transport, Q_0. If h is regarded as a known, independent variable, then Q_0 is known. This Q_0 will be used throughout this study to nondimensionalize Q, and e.g., Eq. (9) becomes

$$\frac{Q}{Q_0} \;=\; F(\frac{h}{d}). \tag{12}$$

A key, implicit assumption of (12) is that the geometric properties of the tank are represented by the single nondimensional variable $h\,/\,d$. In the orifice-only cases, the actual (dimensional) transport Q comes close to Q_0 so that $F(h/d)$ is just slightly less than 1. In other cases, especially those involving long and narrow pipes that will be treated in Sec. 4, Q is much less than Q_0 and so $F(h/d) \;\ll\; 1$.

Summary to here: The objective of the

Experimental observations is to document Q along with the relevant fluid and tank parameters.

Dimensional Analysis is to provide an efficient framework for analyzing the observations.

Modeling is to understand and reproduce the function F of relations like (12).

3.2 A data-driven Model 1

Here is the first example of this procedure — we know all of the individual terms of (12), including Q from the observations of Fig. 2 and Eq. (2). What we do not know is the function F, and dimensional analysis alone can not tell us anything more. To find out what F looks like, evaluate (12) by plotting the nondimensional transport Q/Q_0 against h/d, Fig. 3, left.

It appears that $F(h/d)$ exhibits two regimes.

[6] Evangelista Torricelli, 1608 - 1647, was a student and then a close associate of Galileo Galilei. His experimental investigations on a draining tank showed that the outflowing jet described a ballistic trajectory like that of a solid particle. Torricelli's research on vacuum and barometers led to an appreciation for atmospheric pressure and the crucial insight that 'we live submerged at the bottom of an ocean of air'. This included that horizontal variations of pressure were the immediate cause of winds, the start of dynamic meteorology. A derived unit of pressure, the torr, is in his honor and is 1 torr = 1 mmHg (nominal g) at 0 C. The torr is today used mainly in vacuum applications.

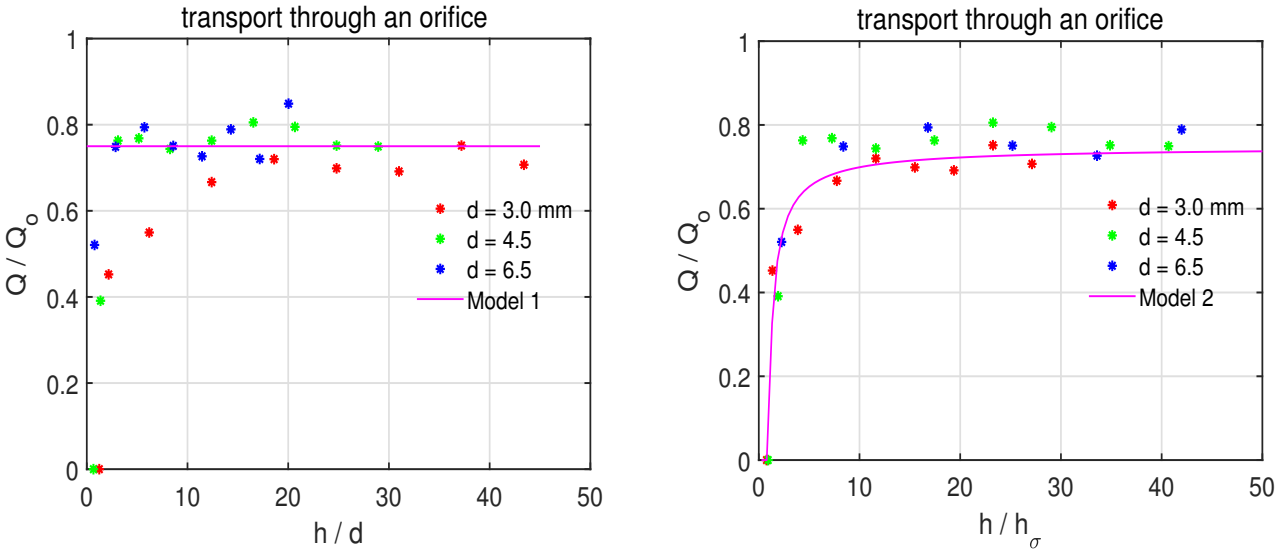

Figure 3: **(left)** Observed volume transport from the orifice-only experiments of Fig. 2. The transport is nondimensionalized consistent with Eq. (12). It is argued that there are two regimes evident here. At small h/d, the nondimensional transport decreases as h/d goes to zero. At larger h/d, the transport is approximately independent of h/d, the magenta line which is Model 1, Sec. 3.2. **(right)** This is the same data shown at left, except that the independent variable is h/h_σ, where h_σ is the pressure head due to surface tension, Eq. (19). This magenta line comes from Model 2 described in Sec. 4.3.

- At smaller values of h/d (small compared to what?), the normalized volume transport goes to zero as h/d goes to zero, and indeed the transport may vanish while h is still appreciable. This is directly related to the surface tension-induced bubble noted above, and discussed further in Sec. 4.
- At larger values of h/d, roughly $h/d > 10$, which includes most of the experimental data, the normalized volume transport is quasi-independent of h/d. In other words, at larger values of h/d, the function $F(h/d)$ is nearly a nondimensional constant, call it C.

Dimensional analysis does not evaluate C, but the data of Fig. 3 indicate that

$$\frac{Q}{Q_0} \;=\; C \;=\; 0.77 \;\pm 0.03 \tag{13}$$

is a reasonable first approximation for these three experiments. It bears some emphasis that the step from Eq. (12) to (13) is

- empirical — C is calibrated using these observations, and 0.77 may not be appropriate to your apparatus or your fluid.
- contingent — Eq. (13) holds only for larger h/d.

The parameter C is called the 'discharge coefficient', and a value in the range $0.6 < C < 0.8$ is expected for simple, square-edged orifices of the present sort.[7]

The physical process that leads to a C that is slightly less than 1 in these experiments is not primarily friction (viscosity), as one might first guess, but rather inertial acceleration on the water approaching the orifice. The evidence for this is twofold. First, C varies only weakly with viscosity (temperature) in this family of experiments. Second, dye observations show that the flow into the orifice comes from the entire hemispherical region inside the tank. The inflow to the orifice has to be accelerated, and some fraction of it also has to make a sharp 90 degree change in direction as it approaches and enters the orifice. Even modest fairing (rounding on the inside of the orifice) can ease this sharp change of direction and bring C close to 1.0. On this basis, the orifice flow process will be called 'inertial' to distinguish from viscous and surface tension phenomena coming in the next two sections.

Given (13), a useful model of the outflow transport, dubbed Model 1, is just

$$\boxed{Q_1 \;=\; C \times Q_0 \;=\; C\,\frac{\pi}{4}\,d^2\,\sqrt{2\,g\,h}.} \tag{14}$$

From here and given Eqs. (1) and (2), it is straightforward to write an ODE for $h(\,t\,)$,

$$\frac{d\,h}{d\,t} \;=\; -\,\frac{Q_1}{A} \;=\; -\,C\frac{d^2}{D^2}\,\sqrt{2\,g\,h} \tag{15}$$

that may be integrated to find

$$h(t) \;=\; \left(\sqrt{h_0} \;-\; \left(0.5\,C\,(\frac{d}{D})^2\,\sqrt{2\,g}\right)\,t\right)^2. \tag{16}$$

This defines a parabolic $h(t)$ (second degree in time) that, overall, bears a striking resemblance to the experimental data shown in Fig. 2 (the dashed, blue line compared to the blue dots). In all cases the surface height decreases rapidly at the start of an experiment and then slows markedly as $h \to 0$. When a pipe is present, friction (laminar viscosity and turbulence) can change the rate quite a lot, but this pattern is characteristic of the $\sqrt{g\,h}$ dependence of a gravity-driven outflow transport, Eq. (11).

Model 1 makes a very good start, and for not much effort. Regardless, there is some room for improvement. Eq. (14) departs from the observations at smaller values of h/d, roughly $h/d < 8$, in that it indicates constant $Q_1/Q_0 \;=\; C$ all the way to h = 0. On the other hand, the observations indicate that the (nondimensional) transport slows for small h/d, and then may stop altogether before the tank is completely drained, Fig. 3. This is not a measurement artifact. The corresponding error in Eq. (16) is that the predicted h goes to zero. Evidently something is missing from (14) and (16).

[7] A thoughtful discussion of C is by Savage, T. Porterfield, W. R. Penney and E. C. Clausen, The draining of a tank: A laboratory experiment in fluid mechanics. ASEE Midwest Section Conference, 2021.

3.3 Problems

- The orifice-only outflow Model 1, Eq. (14), can be rewritten as an ordinary differential equation $dh/dt = F(h, g, d, D)$, Eq. (15). Integrate this equation given an initial value $h(t = 0) = h_0$ to find Eq. (16).[8] How does this solution compare with the expectations from dimensional analysis, Eq. (3)?

- It has been noted that a parabolic trajectory $h(t)$ is characteristic of a gravity-driven outflow for which $Q \propto \sqrt{g\,h}$. Suppose instead that the outflow transport is (for some reason) linear in h, i.e., $Q \propto g\,h$. What is the trajectory $h(t)$ in that case?

- Imagine that the water tank is closed on top, so that the air pressure above the water surface can be altered by a controllable air pump. What additional air pressure (above atmospheric) would be required to yield a constant Q, until the tank drains?

- It was claimed in Sec. 3.2 that the discharge coefficient C for the present experiments is effectively constant because it is a result of inertial (accelerated) flow. This depends upon the geometry of the orifice which doesn't change appreciably from one experiment to the next. It is messy to think about, but suppose that the fluid being drained is honey, which has a viscosity that is from 3000 to 10000 times larger than that of water. How would this increased viscosity affect the magnitude of the transport? Does this imply that C must, in general, depend upon ν, even while the claim made here is that viscosity is not important for *these* orifice-only experiments? (This illustrates why nearly every claim made here has to be qualified with the tedious phrase 'for these experiments'.)

4 Surface tension reduces transport in the small h/d regime

It was noted above that the outflow may come to a stop before $h \to 0$. In that state the outflow appears to be blocked by a flattened bubble of fluid that caps the orifice. The inference is that surface tension has overcome the hydrostatic pressure difference (7) that would otherwise accelerate fluid through the orifice. This is not a large effect on the scales that characterize the parameter range of these experiments, i.e., the d, h, g, etc. However, this effect is systematic and interesting on its own merits.[9]

[8] An excellent tutorial for this problem is https://www.youtube.com/watch?v=iKDdInE7wqE.

[9] Surface physics is vitally important for microfluidic (very small scale) devices. An excellent introduction to surface tension is https://en.wikipedia.org/wiki/Surface_tension Also highly recommended and more advanced is https://web.mit.edu/1.63/www/Lec-notes/Surfacetension/Lecture1.pdf

4.1 Why do fluids exhibit surface tension?

Surface tension is a fundamental characteristic of a fluid that has an appealing microscale explanation. The individual molecules of a fluid are free to move and jostle around but they are also cohesive, in that fluid molecules exert an intermolecular attraction (hydrogen bonding in water) that acts to clump fluid molecules together. When clumped together, water molecules are in a lower energy state than if they were separated and moving independently (as do the molecules that make up a gas). Where there is a free surface that exposes the fluid to some other, less attractive material — if water, then air — the molecules that are immediately on the free surface will not have fluid molecules on all sides, and so will be in a slightly elevated energy state; think of attracting particles that have been pulled apart. The existence of a free surface thus implies some potential energy that may be characterized as a thermodynamic property called surface tension, denoted here by σ. Surface tension can be viewed as either an energy per unit area, in SI units, Joules per meter squared, and so $\sigma \doteq [\,1\;0\;-2\,]$, or, as a force per unit length, Newtons per meter, and having the same fundamental dimensions. Both interpretations are useful.

Water has a fairly high surface tension,

$$\sigma \approx 75 \times 10^{-3}\ \mathrm{J\ m^{-2}} = \mathrm{N\ m^{-1}},$$

compared to most other familiar fluids, e.g., isopropyl alcohol, for which $\sigma \approx 20 \times 10^{-3}$ N m^{-1}. A familiar consequence is that water tends to form into spherical drops (absent some other influence such as air drag on a falling drop) that minimize surface area, and thus the surface energy for a given volume. Surface tension, viewed as a force per unit length, acts as a membrane under tension that maintains a spherical shape. A consequence is that there is an elevated pressure inside a water drop that is proportional to σ times the Laplace curvature of the surface. The curvature of a sphere is $2/r$, with r the radius; the pressure inside a spherical water drop is thus

$$P_{drop} = 2\,\sigma / r \tag{17}$$

higher than the ambient pressure.[9]

4.2 Surface tension and pressure within a cylindrical jet of water

A vigorous outflow through a round orifice produces a cylindrical jet of water, Fig. 1.[10] The surface curvature of a cylinder is half that of a sphere having the same radius and thus the surface-tension

[10] A parcel of fluid within the free-falling jet has a certain horizontal velocity, $dX\,/\,dt = V_o$, that is conserved, and it is accelerated downward by gravity at a rate $d^2\,Y\,/\,dt^2 = -g$. A parcel, and thus the jet, traces a parabolic (ballistic) trajectory, $X \propto (V_o\,/\sqrt{g})\,\sqrt{-Y}$.

induced pressure within the jet is estimated to be half that of the corresponding sphere, i.e.,

$$P_\sigma \;=\; \frac{\sigma}{r}. \tag{18}$$

The pressure P_σ can be expressed as an equivalent hydrostatic pressure head,

$$\boxed{h_\sigma \;= \frac{\sigma}{\rho\, g\, r},} \tag{19}$$

which is constant for a given experiment. For the surface tension of water and if r is a few millimeters, then h_σ is O(1) cm.

From this discussion it seems plausible that the outflow transport might be dependent upon h_σ which suggests a revised form of Eq. (12),

$$\frac{Q}{Q_0} \;=\; F(\frac{h}{h_\sigma}). \tag{20}$$

When the data of Fig. 3 are nondimensionalized in this way (right panel), the normalized transport is found to decrease significantly when $h/h_\sigma < 5$, and vanishes at roughly $h/h_\sigma \leq 1$. This is consistent with the notion that the surface-tension induced pressure inhibits the outflow, an effect which is especially noticeable for the smaller diameter orifices and pipes considered here.

4.3 Model 2 includes a first-order effect of surface tension

This, in turn, suggests a revised model for orifice transport. Model 1, Eq. (14), amounts to taking the pressure outside the tank to be zero. Now we understand that there is a slightly higher pressure required to overcome the surface-tension induced pressure acting upon the jet. With that in mind, revise the Torricelli velocity to

$$V_{T\,\sigma} \;=\; \sqrt{2\,g\,(h - h_\sigma)}, \tag{21}$$

and define a Model 2 for the transport,

$$\boxed{Q_2 \;=\; C\,\frac{\pi}{4}\,d^2\,\sqrt{2\,g\,(h \;-\; h_\sigma)}} \tag{22}$$

that is valid only for $h \;\geq\; h_\sigma$. This may be solved for

$$h(t) \;=\; h_\sigma + \left(\sqrt{h_0 \;-\; h_\sigma} \;-\; \left(0.5\,C\,(\frac{d}{D})^2\,\sqrt{2\,g}\right)\;t\right)^2, \tag{23}$$

the solid red line of Fig. 2. Compared with Model 1 that ignored surface tension (the dashed red line), the new Model 2 solution for $h(t)$ is only slightly different overall from that of Model 1, but it

does include the qualitative feature that h asymptotes to h_σ, rather than to zero, as does the solution of Model 1.

A more sensitive test of Model 2 comes from differentiating the solution (23) and evaluating $Q_2/Q_0 = F(h/h_\sigma)$, the magenta line of Fig. 3. This shows a slowing of the outflow as h/h_σ falls below about 5, and stopping altogether at about $h = h_\sigma$. These are reasonably consistent with the observations, and suggest that this first-order treatment of surface tension is a small but useful step toward a more complete and realistic model.[11]

The first-order treatment of surface tension reflected in Eq. (21) is as far as this study will go regarding surface tension *per se*. This result will be incorporated into Models 4 and 5 developed in Secs. 6 and 7. Until then, surface tension will be set aside in order to focus attention on the viscous effects that can greatly modify the outflow transport through a pipe.

4.4 Problems

- The left and right sides of Fig. 3 give us a chance to compare two versions of a nondimensional format, $F(h/d)$ vs. $F(h/h_\sigma)$ (recall that F merely holds a place for an unspecified function). Which is the better nondimensional independent variable, h/d, or h/h_σ? What criteria could we deploy to decide this? Three suggestions: First, simplicity or transparency are always desirable, but probably not decisive. Second, if one version produces a more convincing collapse of the data toward a single curve, then that would surely count in its favor. Third, which of the inferred relations $F(h/d)$ and $F(h/h_\sigma)$ has a better-motivated, quantitative physical interpretation? Can you show that

$$\frac{h}{h_\sigma} \propto \frac{hydrostatic\ pressure}{surface\ tension\ pressure}.$$

  This ratio of gravitational to surface tension pressure is often called a Bond or Eotvos number.

- Using dimensional analysis, show that the pressure anomaly inside a cylindrical jet of radius r is as given by Eq. (18), $P_\sigma = \sigma\,/\,r$ up to an unknown factor (happens to be 1). Two hints: for surface tension, $\sigma \doteq [1\ 0\ -2]$ and pressure, $P \doteq [1\ -1\ -2]$. Can you go from here to the equivalent height of a hydrostatic pressure and Eq. (19)?

---

[11] The present treatment of surface tension overlooks a detail (within a detail). As h approaches h_σ, the outflow slows markedly, and then begins to dribble down the side of the tank: a weak outflow continues, but there is no more ballistic jet. After a short time, the dribbling stops and the orifice becomes capped over, as described above. The cap has some curvature but not so much as a sphere: $P_{\sigma-cap} \approx \sigma\,/\,r$ seems plausible for the blocked outflow. Also ignored here is the wetting properties of the solid substrate: polypropylene, does it attract or repel water? A single stage surface tension effect estimated by Eq. (22) is perhaps a fortuitous approximation. For more on these phenomena, see Ferrand, J., L. Favreau, S. Joubond and E. Freyssingeas, 2016, Wetting effect on Torricelli's law, Phys. Rev. Lett., 117, 248001 - 248005.

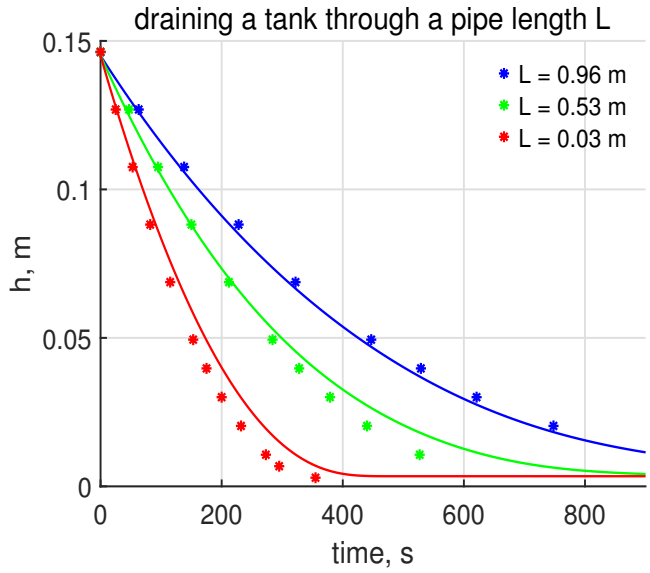

Figure 4: Surface height, $h(t)$, from three experiments in which the water was drained through pipes that had diameter $d = 4.7$ mm and one of three lengths, $L = 0.96$ m, 0.53 m, or 0.03 m, almost an orifice. The solid lines are calculations made by Model 4 discussed in Sec. 6.

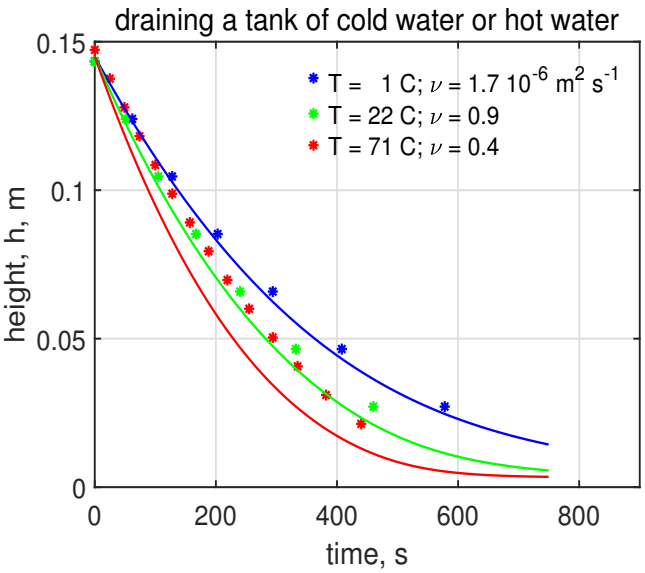

Figure 5: Surface height, $h(t)$, from three experiments that had pipe diameter and length in common, $d = 4.7$ mm and $L = 0.64$ m and thus $L/d \approx 140$. They differed by the temperature of the water, from nearly freezing (blue dots) to very hot (red dots). As a consequence, the kinematic viscosity, ν (= μ/ρ), varied by roughly a factor four. The warmest water (red dots) which had the smallest viscosity, drained considerably faster than did the cold water (not surprising), but, notice that it drained only slightly faster than did the room temperature water (green dots). This hints at something important coming in Sec. 7.2

5 Outflow through an orifice and a pipe, starting with observations

If the outflow must pass through a pipe, as on the cover page, it is expected that the volume transport will be lessened by viscous drag between the moving water and the walls of the pipe. A few experiments show this effect clearly; for a given fluid (water at room temperature) and a given diameter of the pipe and orifice, the tank drains considerably more slowly when the pipe is longer, Fig. 4. By changing the temperature of the water, and thus the viscosity of the water, it is evident that warmer water (smaller viscosity) drains somewhat faster than does colder water, Fig. 5. The qualitative sense of these viscous effects is not surprising. To go beyond that and make a model, we have to define the magnitude of viscous effects. How can we organize the experimental data to this end?

As a guide, let's look for the relationship between the outflow transport and the (presumed) relevant variables under the assumption that the outflow transport is dependent only upon the local conditions at the orifice and the pipe (note that surface tension is omitted from here on until Model 5).

- A VPlist for pressure-driven outflow of water through an orifice and a pipe: (24)

1. outflow volume transport, $Q \doteq$ [0 3 -1], the dependent variable,
2. diameter of the orifice, $d \doteq$ [0 1 0], a parameter,
3. hydrostatic pressure head at the orifice, $g\,h \doteq$ [0 2 -2], an independent variable,
4. kinematic viscosity of the water, $\nu \doteq$ [0 2 -1], a parameter,
5. length of the pipe, $L \doteq$ [0 1 0], a parameter.

Three nondimensional variables are expected, and for this (arbitrary) ordering of the VPlist, the algorithm returns

$$\frac{Q}{L\,\nu} = F(\frac{d}{L}, \frac{L^2\,gh}{\nu^2}). \tag{25}$$

This is correct mathematically, i.e., it is a basis set of nondimensional variables for this VPlist. However, the important scale that normalizes the transport, $L\,\nu$, seems oddly out of place here. ($L\,\nu$ will arise again later in a context where it will make sense.) For now, we would prefer the physically sensible zero-order model defined by Eq. (11), $Q_0 = \frac{\pi}{4}d^2\sqrt{2gh}$. This is a reminder that the purely formal method of dimensional analysis may not provide what we would recognize as physical sense; that is left for us. After some reorganizing of the variables in (25) there follows an important relationship:

$$\boxed{\frac{Q}{Q_0} = F\left(\frac{L}{d}, \frac{V_T\,d}{\nu}\right)} \tag{26}$$

The left side of (26) is the now familiar nondimensional volume transport. The unknown function F on the right-hand side depends upon two nondimensional, independent variables. The first independent variable, $L\,/\,d$, is an aspect ratio, and is a straightforward reply to 'how long is this pipe?' given in natural units. In these experiments, L/d is in the range 0 - 500. The second nondimensional variable on the right side of (26) is less obvious.

5.1 Reynolds numbers, external and internal, Re_x and Re

The second independent variable

$$Re_x \;=\; \frac{V_T\, d}{\nu} \tag{27}$$

has the form of a

$$Reynolds\ number \;\propto\; \frac{velocity\ scale \times length\ scale}{kinematic\ viscosity} \tag{28}$$

This ratio is important in many contexts, and Reynolds numbers come in correspondingly many versions.[12] The terms of (27) are:

- ν**, kinematic viscosity**, is straightforward when it is regarded as a fluid property, the usual intent of the Navier-Stokes equations.
- V_T**, a velocity scale** (a speed) is usually clear. In Eq. (28) the velocity is the Torricelli velocity, $V_T \;=\; \sqrt{2\,g\,h}$, which may be evaluated *a priori*, before a solution is known, presuming that h is observed or otherwise known. For that reason the ratio (28) is said to be an 'external' Reynolds number. This Re_x is different from the much more often encountered

$$\text{internal Reynolds number,} \quad Re \;=\; \frac{V_a\, d}{\nu}, \quad \text{where} \quad V_a \;=\; \frac{Q}{a} \tag{29}$$

  The velocity V_a is the area-averaged velocity in the pipe and is known only after we know Q and so Re of Eq. (29) is said to be 'internal'. The bridge between these Reynolds numbers is

$$Re \;=\; Re_x \frac{Q}{Q_0} \tag{30}$$

  and hence Re will be somewhat smaller numerically than is Re_x. The internal Reynolds number will be used extensively in Sec. 7 when this analysis makes connection with the extensive historical literature on pipe flows.

[12] An excellent discussion of the Reynolds number including an interesting history is https://en.wikipedia.org/wiki/Reynoldsnumber

- L**, a length scale,** here taken to be the pipe diameter, d. The length scale is often the least obvious term in a Reynolds number. A conventional (though not altogether convincing) way to develop an interpretation of the length scale comes from a scaling analysis of the Navier-Stokes momentum equation,

$$\frac{\partial \mathbf{V}}{\partial t} \; + \; (\mathbf{V} \cdot \nabla)\, \mathbf{V} \; = \; -\nabla P/\rho \; + \; \nu \nabla^2 \mathbf{V} \; + \; \mathbf{g}. \tag{31}$$

  The goal is to compare the magnitude of the viscous term (second term on the right) to the inertial, acceleration term (second term on the left). Let V be the velocity scale, an upper bound on the magnitude of the fluid velocity expected in the problem. The kinematic viscosity ν can remain as is. The key is to identify a length scale, X, over which this velocity varies by O(1) so that, say for the x direction,

$$\frac{\partial V}{\partial x} \; \propto \; \frac{V}{X} \quad \text{and} \quad \nabla^2 \mathbf{V} \; \propto \; \frac{V}{X^2}.$$

  Under the assumption that a single length scale X is appropriate to the spatial derivatives in both the inertial term and the Laplacian of the viscous term, then it is straightforward to estimate the ratio of the inertial term(s) and the viscous term;

$$\frac{inertial}{viscous} \; \propto \; \frac{(\mathbf{V} \cdot \nabla)\, \mathbf{V}}{\nu \nabla^2 \mathbf{V}} \; \propto \; \frac{V^2/X}{\nu\, V/X^2} \; = \; \frac{V\, X}{\nu} \; = \; Re,$$

  a Reynolds number. In the case of pipe flow being considered here, the velocity varies with the radius, mainly, and thus the length scale X is identified as d.

Interpretation of Re_x: It is reassuring to find that a nondimensional number comes out to be O(1), as that implies a comparison of like things. There is no such comfort here; the numerical values of Re_x are O(10^4) (which is typical also for the Re of intermediate scale pipe flows). Taken literally, this would imply that the possible viscous force is much, much less than the inertial forces, and that some other term in the Navier-Stokes momentum balance must account for inertial accelerations (pressure gradient and/or time dependence). That is true, but nevertheless, these very large Re_x should not be interpreted to mean that viscosity may be omitted altogether (reminiscent of the air flow around a golf ball or a soccer ball, Sec. 4.5 of the main text).

What is the interpretation of Re_x for the present experiments? First, note that Re_x is the only independent variable of Eq. (26) holding ν; whatever viscous effects there are will be attributed to Re_x-dependence. Within this family of experiments, we can expect that a smaller value of Re_x should correspond to greater viscous effects, *viz.*, reduced transport.[13] The external Reynolds number thus appears to be a rough comparative measure of the ratio of inertial force (accelerations) to

[13] We usually think of a Reynolds number in association with viscous effects, but notice that viscosity happens to be in the denominator (it could have been otherwise). With that convention, smaller ν gives large Re, all else equal.

viscous force. Finally, given Eq. (30), the present Re_x can easily make contact with the vast literature on pipe flows that rely on the internal Reynolds number, Re (more on this in Sec. 7).

5.2 The function F for orifice plus viscous pipe flow

The relation (26) may be evaluated from the experimental data to provide a look at the function, $F(L/d,\ Re_x)$, Fig. 6. The coordinate system is three-dimensional since there is one nondimensional dependent variable, Q/Q_0, and two nondimensional independent variables, L/d, and Re_x, as noted above. (Notice that there is no mention of surface tension.)

A given experiment returns a handful of data points, all at the same L/d, and sampling a range of h, starting from h_0 and going to smaller h, in some experiments, to h_σ. The data points from a given experiment thus line up in strings that run parallel to the Re_x axis; larger Re_x is due to larger h. The nondimensional transport within a given experiment decreases smoothly with decreasing Re_x and thus with decreasing h. This is qualitatively consistent with the expectation that smaller Re_x (in the case of a single experiment because of small h) will generally correspond to a greater viscous effect.

The amplitude of the viscous effect, i.e., the decrease of the transport, depends also upon L/d. For the smallest values of L/d found on the left-most part of Fig. 6, this becomes the orifice-only result that $Q/Q_0 \ = \ C \ \approx \ 0.77$. In that limit, the Re_x-dependence vanishes: if L vanishes, then viscous effects effectively vanish as well. The converse is just as true; for a given Re_x, the nondimensional transport decreases significantly with increasing L/d; the decrease is especially strong at small values of L/d. In the range $L/d \ \approx \ 400$ and smaller Re_x found in the lower right corner of Fig. 6, the nondimensional transport is only about 25% of the orifice-only value, C.

It appears that the nondimensional coordinates of Eq. (26) make a useful summary of the transport dependence upon h, L, d and ν. Once we know this dependence we can write an ODE for the surface height,

$$\frac{dh}{dt} \ = \ - A^{-1} Q_0 F(\ L/d,\ Re_x\ ), \tag{32}$$

a generalized version of Eq. (15). The Re_x in the argument of F above will include h. This will likely frustrate a separation of variables, but numerical solution should be fast and accurate. To implement such a solution, the function F has to be made portable. One could estimate an empirical fit to a dataset like Fig. 6, or, seek an appropriate model.

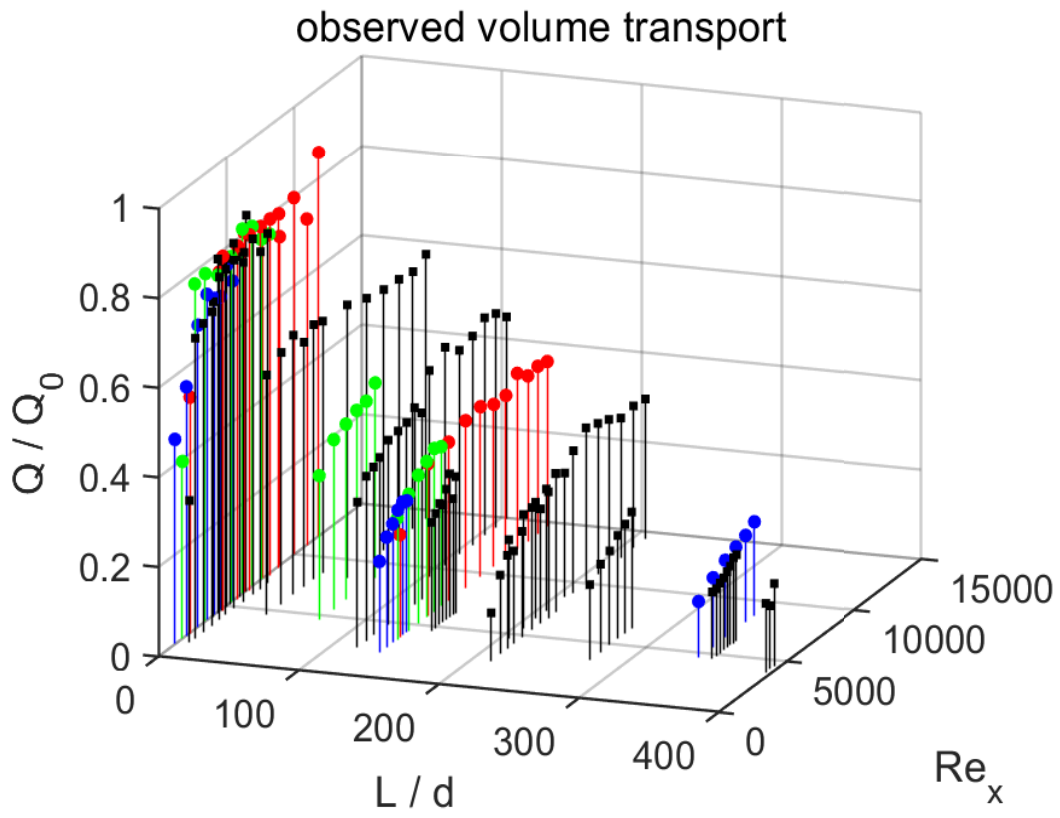

Figure 6: Observed nondimensional volume transport as a function of the pipe aspect ratio, L/d, and the external Reynolds number, $Re_x = V_T\, d\,/\,\nu$. There are 23 experiments shown here, each of which yields between five and 12 data points; 181 points in total. The data from a given experiment line up in a string that has a constant L/d, but a varying h. Each experiment thus samples a small range of Re_x. The red, green and blue dots are the data from the nine experiments of Figs. 2, 4 and 5. The black dots are from fourteen other, similar experiments. This is a rather dense and complex figure, but if you study it for just a minute you can envision that the locus of data points implies a two-dimensional surface $F(L/d,\ Re_x)$. A key objective of this study is to understand how such a surface arises and to use that understanding as a guide to model development coming in Secs. 6 and 7. These data and a Matlab script to read and plot them are linked in Sec. 8.

5.3 Problems

- Fig. 6 includes all of the data taken in these experiments, including data at small $h \,/\, h_\sigma$ that were likely affected by surface tension as noted in the previous section. There is no accounting for surface tension effects in the coordinate system of Fig. 6, and so it is questionable whether they should be included. Where in Fig. 6 (at what L/d and Re_x) are these surface-tension-affected data?
- Can you find and then interpret the data that came from the three experiments with variable temperature shown in Fig. 5?
- Using the properties of a null space basis, recast Eq. (25) into the form preferred here, Eq. (26). The key step is choosing a scale for the dependent variable.

6 Models of viscous, laminar pipe flow

This section will develop models of laminar flow that are appropriate for the lower Re_x range of the parameter space sampled here, roughly $Re_x \leq 7000$. It is expected that at larger Re_x there will be a transition from laminar to turbulent flow with a consequence of larger wall stress (for a given Re_x) than would be predicted by a laminar flow model. More on this in Sec. 7.

6.1 Poiseuille's solution for laminar flow, Model 3

For now, consider pipe flow alone, ignoring the necessity of a tank and orifice, and omitting surface tension. Suppose that the pressure at the ends of this horizontal pipe are known and that the pressure difference is δP_{pipe}. Additionally, assume that the flow is unchanging along the pipe, and said to be fully developed.[14] In that case the pressure gradient, a force per unit volume, is

$$\frac{\partial P}{\partial x} = \frac{\delta P_{pipe}}{L},$$

and also uniform along the pipe. Given the pressure gradient, what is the volume transport through the pipe?

[14]The strong acceleration of flow through the orifice and into the pipe is bound to cause some disturbance that may damp out with distance downstream. The distance downstream required to lose memory of the orifice is called the entry length; the equilibrated flow further downstream is said to be fully-developed. The effect of a finite entry length is likely to be increased drag overall. There is some evidence of that in this dataset, but it is small compared to the effects of turbulent flow taken up in Sec. 7.

- A VPlist for the pressure-driven transport of a fully-developed, viscous pipe flow: (33)

1. volume transport, $Q \doteq$ [0 3 -1], the dependent variable,
2. pressure gradient, $\partial P/\partial x \doteq$ [1 -2 -2], an independent variable,
3. radius of the pipe, $r \doteq$ [0 1 0], a parameter,
4. dynamic viscosity, $\mu \doteq$ [1 -1 -1], a parameter.

This is a subset of the VPlist that led to Eq. (26). In this VPlist there are four dimensional variables having three fundamental units, and hence there is just one nondimensional variable, the nondimensional transport, that must be a constant,

$$\frac{Q\,\mu}{r^4\;\partial P/\partial x} \;=\; constant. \tag{34}$$

The result (34) from dimensional analysis has the form of the famous and very useful Poiseuille solution for the transport of a laminar, fully-developed, viscous pipe flow,

$$\boxed{Q_3 \;= \frac{\pi}{8}\,\frac{r^4\;\delta P_{pipe}}{\mu\;L},} \tag{35}$$

also called the Hagen-Poiseuille solution.[15] This is taken to be Model 3. Two things to note: 1) the sensitive dependence upon r, here r^4 compared with r^2 for an inviscid, inertial orifice flow of Sec. 3, and, 2) the transport is linear (directly proportional to) the pressure gradient. This seems plausible, but is not always the case as we will see in Sec. 7. Poiseuille's[16] solution for laminar pipe flow is closed, including the leading factor $\pi/8$ that is needed to calibrate the dimensional analysis result, (34).[17] After some rearrangement, the transport (35) can be rewritten in a nondimensional form using the zero-order model of Eq. (11) to scale the dependent variable,

$$\boxed{\frac{Q_3}{Q_0} \;=\; \frac{1}{64}\,(\frac{L}{d})^{-1}\,Re_x} \tag{36}$$

[15]The dimensional analysis leading to (34) is standard fare and is useful for now. However, its success in yielding the Poiseuille relation owes to an arbitrary choice in the variables of the VPlist (33) that will be discussed further at the end of Sec. 7.

[16] Jean L. M. Poiseuille (1797 - 1869) was a French physiologist who pioneered the quantitative study of blood flow. He discovered the Poiseuille relation for viscous flow in pipes (blood vessels) experimentally. Some years later he provided the corresponding theory, including Eq. (35), one of the first complete solutions of the Navier-Stokes equations. His contributions also include the development of practical instruments for measuring blood pressure *in vivo*. The CGS unit of dynamic viscosity is the poise, P, in his honor; 1 P = 0.1 N s m^{-2}.

[17] The derivation of (35) is useful to see and can be found in most fluid mechanics texts. A very good online reference is https://en.wikipedia.org/wiki/Hagen-Poiseuille_equation

Under the conditions of its derivation, fully-developed laminar flow, the Poiseuille solution gives a very good account of experimental observations. Indeed, it works well enough that it may be used along with careful measurements to estimate fluid viscosity, μ. Does (35) suffice for the experimental configuration used here? We can learn a lot by plotting the Poiseuille solution in the coordinates of Fig. 6 (Fig. 7, upper right). This shows some promise in the range of smaller Re_x and larger L/d, which implies large viscous effects. But at larger Re_x and smaller L/d, the Poiseuille solution diverges, predicting transport that is much larger than the transport that could be accelerated through the orifice by the given pressure difference. The conclusion has to be that the Poiseuille solution taken alone, Eq. (35), Model 3, does not make a suitable model of the present system — tank, orifice, pipe, discharge into air. (No doubt M. Poiseuille could have told us as much, even without the hindsight of a fancy diagram.)

6.2 A hybrid Model 4 – Sig. Torricelli, say hello to M. Poiseuille

The fluid path from the tank to the open air can be envisioned in three parts: first, inertial (accelerated) flow from the tank into the orifice; second, viscous (and possibly turbulent) flow through a pipe; and third, escape into the open air and production of a free surface. Each of these has been discussed in isolation, and now we will seek to connect them to make a model of the system as a whole. The idea will be to ensure that the pressure is continuous from the tank to the open air, and that the transport is consistent with the pressure changes and is constant throughout.

Let the pressure across the orifice be $\rho\, g\, h \;-\; P_x$ where P_x is the unknown pressure post-orifice, or right at the start of the pipe. The transport through the orifice will then be estimated as

$$Q_{orf} \;=\; C\pi r^2\sqrt{2(g\, h \;-\; P_x/\rho)}. \tag{37}$$

This pressure difference and thus the transport through the orifice will be less, and possibly a lot less, than the orifice-only Model 1 of Sec. 3, which took the pressure P_x just beyond the orifice to be zero.

The pressure at the end of the pipe is $P_\sigma \;=\; \sigma/r$, the surface tension-induced pressure on the escaping jet of water in contact with air. The transport through the pipe will be estimated from Poiseuille's relation,

$$Q_{pipe} \;=\; \frac{\pi\, r^4}{8\,\mu\, L}(P_x - \frac{\sigma}{r}). \tag{38}$$

The one unknown in this is P_x, the pressure at the start of the pipe. This can be solved by requiring that the transport must be continuous,

$$Q_{orf} \;=\; Q_{pipe}. \tag{39}$$

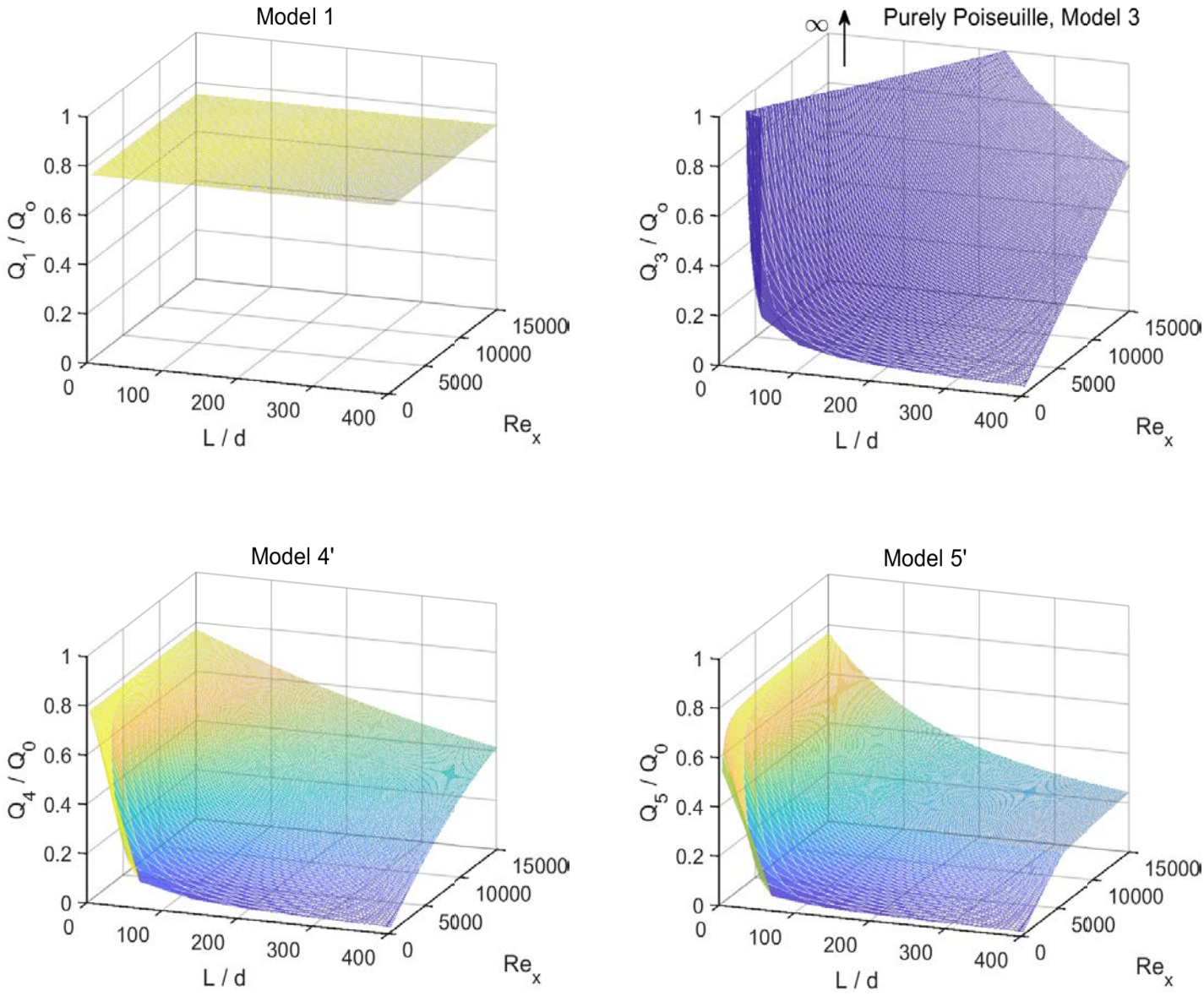

Figure 7: Four models of Q/Q_0 in the independent coordinates L/d and Re_x used in Fig. 6. This necessarily omits reference to surface tension. **Upper Left** The elementary Model 1 solution for transport through an orifice, dubbed Q_1. This solution does not depend upon L or ν and so this model defines a flat plane in this coordinate system. **Upper Right** The Poiseuille solution Q_3 for steady, fully-developed pipe flow. The transport diverges for small L/d and large Re_x, i.e., in the parameter range of smaller viscous effects, and has been clipped at 1. **Lower Left** The solution of Model 4' that combines Torricelli and Poiseuille, Eq. (41) and so has transport that is consistent with both orifice and viscous pipe flow (discussed in Sec. 6.2). The prime indicates that surface tension has been omitted. **Lower Right** Model 5' is similar to Model 4' at left, but includes a correction for the greater wall stress that occurs when the flow is turbulent at larger Re_x (Sec. 7). Notice the difference between Model 4' and Model 5', especially at larger Re_x.

Let

$$p \;=\; \frac{P_x}{\rho}, \qquad S \;=\; \frac{r^2}{8\,C\,\nu\,L}, \quad \text{and recall} \quad h_\sigma \;=\; \frac{\sigma}{\rho\,g\,r} \quad \text{and} \quad \nu \;=\; \frac{\mu}{\rho},$$

in which terms the continuity of transport (39) becomes

$$\sqrt{2(g\,h \;-\; p)} \;=\; S\,(p \;-\; g\,h_\sigma).$$

Squaring and rearranging into a quadratic in p gives

$$S^2\,p^2 \;+\; (2 - 2\,S^2\,g\,h_\sigma)\,p \;+\; S^2\,g^2\,h_\sigma^2 \;-\; 2\,g\,h = 0. \tag{40}$$

Once this is solved for $p \;=\; P_x/\rho$ (the positive root) the transport may be evaluated from either (37) or (38). This model and solution are called Model 4 and Q_4.

When surface tension is included, the analytic expression for Q_4 is too complex algebraically to be useful (though readily evaluated numerically in Sec. 6.4). For now, simplify by setting $h_\sigma \;=\; 0$ so that we can examine the orifice plus viscous pipe flow component, which will be dubbed Model 4'. The pressure, p, is then

$$p \;=\; \frac{P_x}{\rho} \;=\; \frac{-1 \;+\; \sqrt{1 \;+\; 2\,g\,h\,S^2}}{S^2}.$$

Substituting into (38), and after considerable rearranging:

$$\frac{{Q_4}'}{Q_0} \;=\; C\left(\,(\,1 \;+\; 1024\,C^2\,E^2\,)^{1/2} \;-\; 32\,C\,E\,\right), \tag{41}$$

where

$$E \;=\; \frac{L}{d}\,Re_x^{-1}. \tag{42}$$

The Model 4' solution, Fig. 7, lower left, is similar to the Model 3 Poiseuille solution for smaller values of the Reynolds number, roughly $Re_x < 2000$ where viscous effects are most important. It is qualitatively different at larger Re_x where the Model 3 solution diverges. The Model 4' solution gives reasonable transport in that regime because it has included the very important constraint imposed by the necessity for accelerated, inertial flow from the tank and into the orifice.

6.3 A collapse to one independent variable

The Model 4' solution (41) has the interesting property that it depends upon a single, independent nondimensional variable, E, vs. the $L\,/\,d$ and Re_x separately that we learned from dimensional analysis. The nondimensional variable E includes all of the important parameters that are expected to contribute to $Q\,/\,Q_0$ in these experiments (except for σ). A dependence upon the single

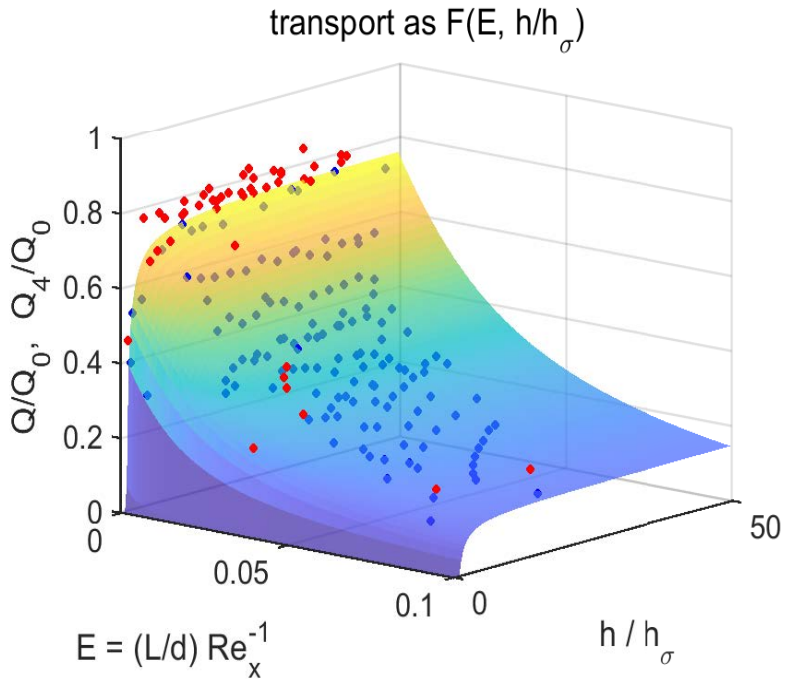

Figure 8: This surface is the Model 4 solution evaluated from Eq. (40), and the points are the full set of observations. The data points that lie below the surface are blue; those above the surface (a distinct minority) are red. The overall shape of the model surface looks reasonable compared to the data, but there is a clear tendency for Model 4 to overestimate transport. A more quantitative comparison comes in the next two figures.

nondimensional variable E is a special case of the more general result from dimensional analysis that indicated two separate, independent nondimensional variables, $L\,/\,d$ and Re_x. This important difference arises because Model 4 was built upon three physical constraints — continuity of volume transport, a solution for orifice flow, and Poiseuille's solution for laminar pipe flow — that were not incorporated into the VPlist (24). Thus the result from dimensional analysis is more general, i.e., less specific, than is the solution of a model that is otherwise consistent with the VPlist. This is a characteristic of dimensional analysis.[18]

The Eqs. (41) and (42) are somewhat surprising, and, if consistent with the observations, useful as well. To find out whether this holds within the observations we need only plot the usual $Q\,/\,Q_0$ against E and find a moderately good correlation, Figs. 8 and 9. It is always desirable to find the most compact description of a dataset or model solution, and this new version (new compared with the three-dimensional presentation of Fig. 6) meets that criterion.

The E description may be readily interpreted as the ratio of two time scales:

$$E \;=\; \frac{L\,/\,V_T}{d^2\,/\,\nu} \;\propto\; \frac{advection\ time}{diffusion\ time}. \tag{43}$$

The numerator is the time required for advection over the length of the pipe L at the speed V_T, and

[18]This important lack of specificity (or unintentional generality) is inherent to dimensional analysis and is discussed in greater depth in the main text, Sec. 3.

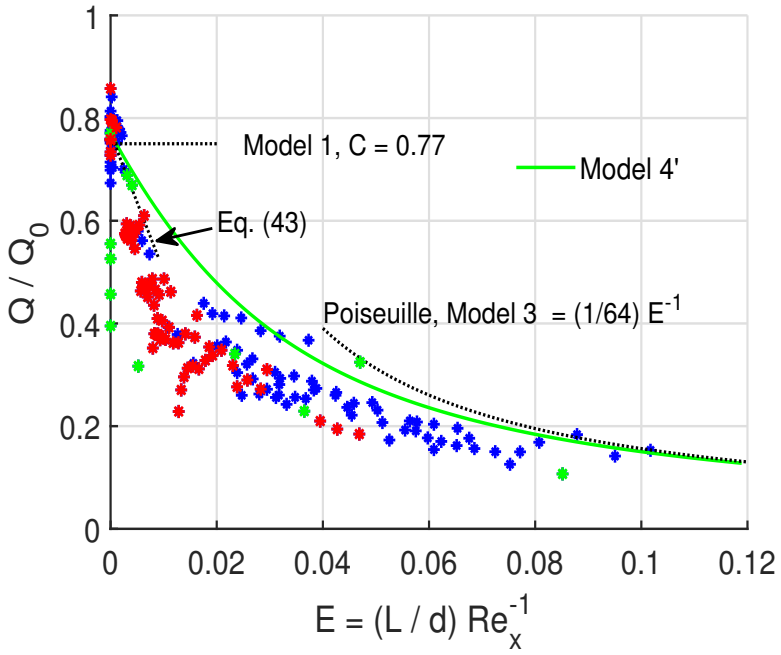

Figure 9: Observed transport (colored points) as a function of a single independent variable, $E = (L/d)\, Re_x^{-1}$. This is a projection of Fig. 8 onto a Q vs. E plane. The green line is the solution of Model 4' (which omits surface tension). The red data points have large Re_x, and the green data points are at small h/h_σ and likely affected by surface tension. The black dotted lines are the asymptotes of Q_4' for small and large E. Notice that the Model 4' solution parallels the data cloud, but sits above it, i.e., Model 4' systematically overestimates the transport, as noted in the previous figure. This will be addressed in Sec. 7.

the denominator is the time required for diffusion across the diameter of the pipe. If the time required for diffusion is comparatively large, then E is comparatively small and viscous effects should be less prominent. This is consistent with the observations.

The function $F(E)$ of Eq. (41) in Fig. 9 is not particularly transparent, but it does have familiar asymptotes, Eq. (44), (45), and (46), that are sketched onto Fig. 9 as dashed, black lines.

- At $E = 0$, where there is no effect of viscosity,

$$Q_4/Q_0 = 0.77 = C. \tag{44}$$

  This is Model 1, inertial, orifice flow.

- At small values of E, which corresponds to small (but not zero) viscous effects, the Model 4 solution goes to

$$Q_4/Q_0 \rightarrow C\left(1 - 32\,C\,E + 512\,C^2\,E^2 \ldots.\right). \tag{45}$$

  This indicates a strong decrease of transport with increasing L that is indeed observed for shorter pipes.

- At large E and large viscous effects,

$$Q_4/Q_0 \rightarrow \frac{1}{64}\,E^{-1}, \tag{46}$$

which is the Poiseuille solution for viscous, laminar pipe flow, and Model 3.

6.4 Model 4 includes surface tension and viscosity appropriate to a laminar flow

Now consider the solution of Eq. (40) with surface tension included, called Model 4 (no prime). The VPlist for this model is

- A VPlist for pressure-driven outflow of water through an orifice and a pipe: (47)

1. outflow volume transport, $Q \doteq$ [0 3 -1], the dependent variable,
2. hydrostatic pressure head at the orifice, $g\,h \doteq$ [0 2 -2], an independent variable,
3. diameter of the orifice and pipe, $d \doteq$ [0 1 0], a parameter,
4. length of the pipe, $L \doteq$ [0 1 0], a parameter.
5. kinematic viscosity of the water, $\nu \doteq$ [0 2 -1], a parameter,
6. surface tension of the water, $\sigma \doteq$ [1 0 -2], a parameter,
7. density of water, $\rho \doteq$ [1 -3 0], a parameter.

A basis set of nondimensional variables is, after considerable rearranging,

$$\frac{Q_4}{Q_0} \;=\; F(\frac{L}{d},\, Re_x,\, \frac{h}{h_\sigma}). \tag{48}$$

If the E-collapse discussed just above is applicable here as well, then provisionally,

$$\frac{Q_4}{Q_0} \;=\; F(E,\, \frac{h}{h_\sigma}). \tag{49}$$

To test whether this is valid we can make a three-dimensional graph of the Model 4 solution alongside *all* of the data, Fig. 8. The surface defined by Model 4 shows the variation of the nondimensional transport with E that could have been anticipated from Fig. 9; it also reveals a sharp decrease in the transport as $h/h_\sigma \to 1$ due to surface tension. This could have been anticipated from Fig. 3, right.

The Model 4 solution makes a plausible qualitative comparison with the observations, Fig. 8, including at small $h\,/\,h_\sigma$. It may be compared quantitatively with the full dataset and returns a coefficient of determination R^2 = 0.74. If the data that have large external Reynolds numbers, $Re_x \geq 7000$, are excluded from the sample, then $R^2 = 0.86$. This is a more appropriate test of this laminar flow model.

Model 4 accomplishes most of what we set out to do in Sec. 1.2: it is understandable, and it gives reasonable (by no means perfect) predictions. It might be appropriate to thank Sig. Torricelli

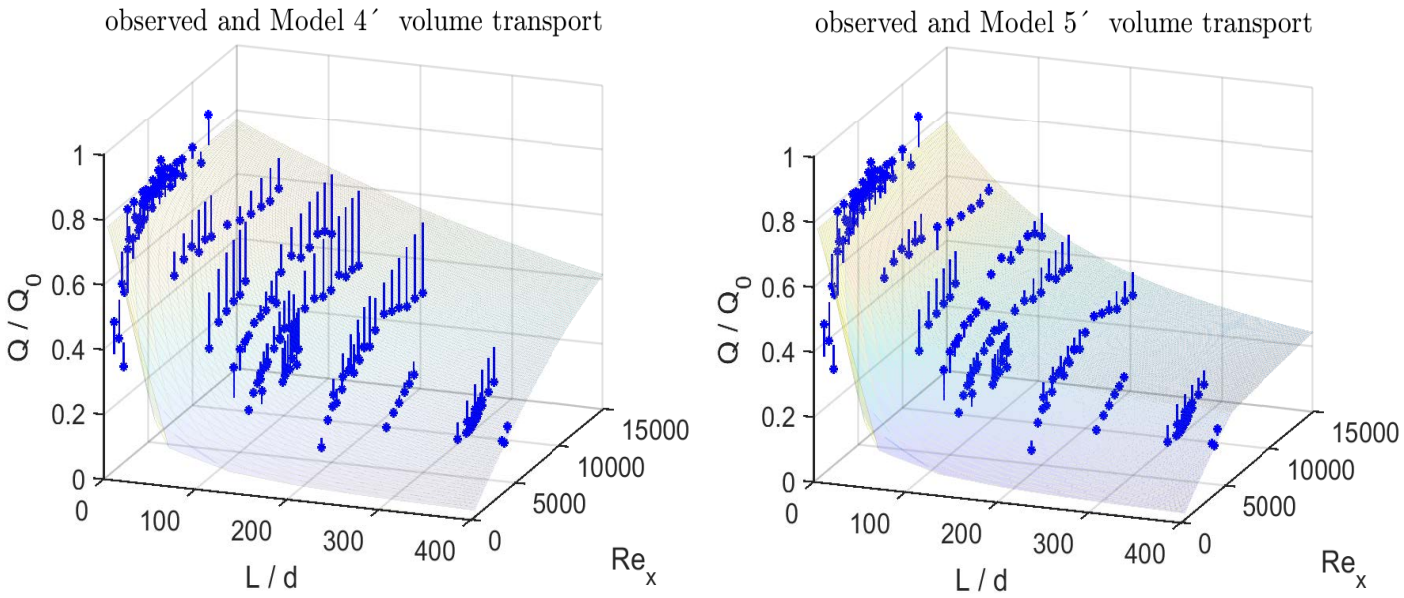

Figure 10: **(left)** Observed volume transport, blue dots, and the Model 4' solution shown as a surface in coordinates $(L\,/\,d,\ Re_x)$ as in Fig. 6. The stem goes from the data point up or down to the surface. This makes it especially clear that Model 4 overestimates transport (underestimates wall stress) at larger values of Re_x. This plot includes all of the data, including data taken at small $h\,/\,h_\sigma$ where surface tension effects are important. The model solution shown in these coordinates has to take $\sigma = 0$ and so can not replicate the reduced transport at very small h and small Re_x. **(right)** This is the same data shown at left, but here the surface is from Model 5' discussed in Sec. 7. The overestimate of transport seen at left is reduced considerably.

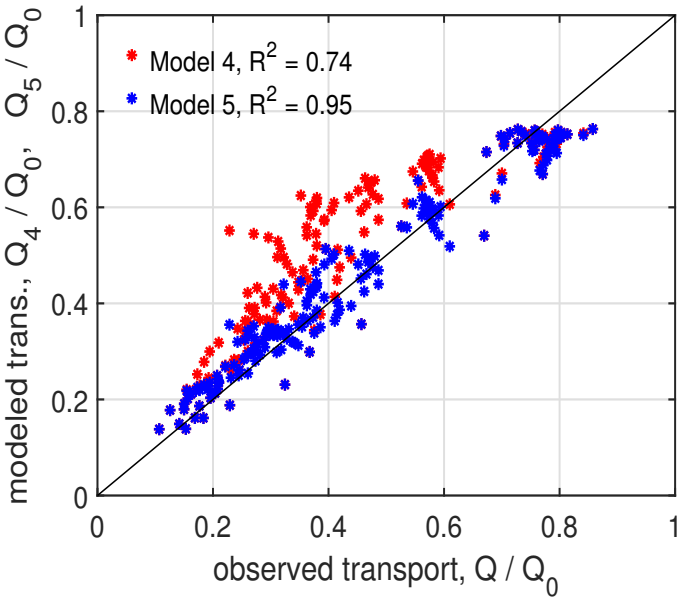

Figure 11: Modeled vs. observed transport. There are two versions of the modeled transport, the red dots are from Model 4 and the blue dots are from Model 5. Notice that Model 4 has a noticeable positive bias (predicts excess transport). This is mostly cured by the changes made to get Model 5, discussed in Sec. 7.

and M. Poiseuille for their remarkable contributions, and stop here. Except for one issue: Model 4 overestimates transport by a noticeable amount, as much as 35% in some regions of parameter space. We have one more step to take.

6.5 Problems

- Starting with the Poiseuille solution, Eq. (35), recast into the nondimensional coordinates of Fig. 6. Show that the Poiseuille solution is (this repeats Eq. (36)),

$$\frac{Q}{Q_0} \;=\; \frac{1}{64}\,(\frac{L}{d})^{-1}\,Re_x.$$

  How does this compare with the surface plotted in Fig. 7, upper right?

- The pipes in these experiments were maintained in a horizontal orientation so that we wouldn't have to consider the angle from horizontal as yet another variable. Now imagine that the discharge end of the pipe was tipped up slightly. How would this affect the transport of the outflow? Can you connect this with the treatment of surface tension in Sec. 4?

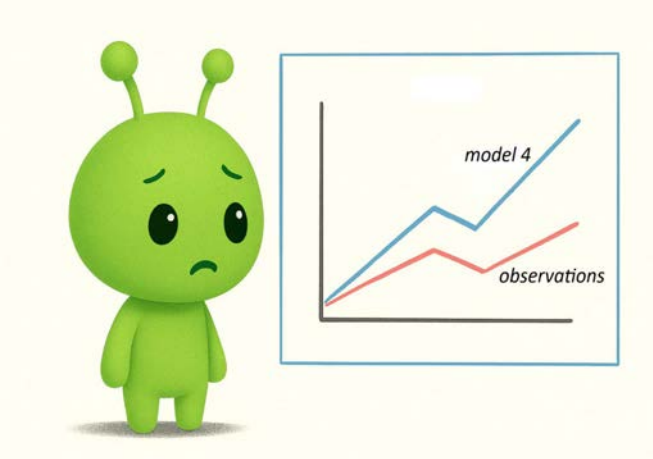

Planetary Explorer testing a new model.
Image by the author using ChatGPT-5.

Make a model, then test a model.

Models flow with grace.
Real, twisting fluids say no!
Try and try again.

7 Turbulent flow and Model 5

The aim of this section is to build a Model 5 that will resolve the systematic overestimation error made by Model 4. This proceeds in four steps:

7.1) Identify the source of the error — the onset of turbulent flow — based in large part upon its dependence upon Reynolds number.

7.2) Review historical analyses that document pressure/velocity correlations in laminar and turbulent pipe flows.

7.3) Use historical analysis to estimate a turbulence-enhanced effective viscosity that may be used within the laminar flow framework of Model 4.

7.4) Test the resulting Model 5 against observations.

7.1 The inferred source of the overestimation error

The error made by Model 4 has a telling geography, being most apparent for the largest Re_x, greater than about 7000, Fig. 10, left. A clear example of this comes from the three experiments of Fig. 5 that showed dependence of Q upon viscosity (due to different water temperature). The two

experiments having cold and room temperature water sampled $2000 \leq Re_x \leq 7000$ and were predicted fairly well by the laminar flow Model 4, Fig. 12. The hot water experiment sampled $4000 \leq Re_x \leq 17000$ and in that range the Model 4-predicted transport exceeds the observed transport by an appreciable fraction, up to 35% at the largest Re_x. This discrepancy easily exceeds the uncertainty on observed Q, and it is systematic, a similar pattern is evident in other experiments that sampled larger L/d and Re_x. The upper Re_x limit for validity of the laminar flow Model 4 appears to be roughly $Re_x \approx 7000$. Using Eq. (30), this corresponds to an internal Reynolds number, $Re = V_a\, d\,/\,\nu = (Q\,/\,Q_0) \times Re_x = 0.35 \times 7000 \approx 2500$, where $Q\,/\,Q_0 = 0.35$ has been read from Fig. 12. A transition from laminar to turbulent flow at roughly this internal Reynolds number is consistent with well-known stability properties of pipe flow.[19] [20] Below $Re \approx 2000$, a laminar pipe flow will be stable, unless strongly perturbed by an outside agent; above a Reynolds number of about 3000, a laminar pipe flow will be unstable and likely to become at least intermittently turbulent. The overestimation of transport by Model 4 thus appears to be linked to the occurrence of turbulent flow.

Turbulence continually mixes higher velocity fluid from the central core of the pipe into the boundary layer on the pipe walls. In a laminar flow the same process occurs by the generally much slower mechanism of molecular diffusion of momentum. Turbulent flow thus results in a higher wall stress than is found in the corresponding (same transport) laminar flow. For a given pressure difference, turbulent flow thus leads to reduced transport, which can be observed directly in Fig. 12 where the transport is nearly independent of Re_x at larger values of Re_x. In contrast, if the flow was laminar, then we would expect a more or less linear increase of Q with Re_x, Eq. (36), which is evident in observations made at smaller Re_x.

7.2 Historical, experimental observations of pipe flow

There are significant engineering and economic consequences that follow from the increased flow resistance caused by turbulence, and the related phenomena have been studied intensively for more than a century and a half.[21] And yet, as Richard Feynman noted in the 1960s, "What we really can

[19] An excellent introduction to turbulent pipe flow (and fluid mechanics generally) is the text by White, F. M. and H. Xue, 2021, 'Fluid Mechanics', 9th Ed., McGraw Hill.

[20] When discussing a change from laminar to turbulent flow it is almost irresistible to speak of a 'transition to turbulent' flow, as done here, even though what actually happens in these experiments is a change in time from (in some cases) turbulent flow to laminar flow as the surface height, h, and the actual velocity Va decrease. This propensity for 'transition to turbulence' may be partly alliteration, but also conceptual; it is much easier to envision going from a known state, laminar flow, into a chaotic state, turbulent flow vs. the other way around. Stability studies must proceed that way. Does it matter which way the transition goes? Is their hysteresis? Probably yes, especially when, as here, the Reynolds number is not far from the transition region.

[21] If turbulence is a new or unfamiliar concept, then a highly relevant, must-see resource is the film by R. Stewart, 'Turbulence', available online at https://hml.mit.edu/ncfmf/

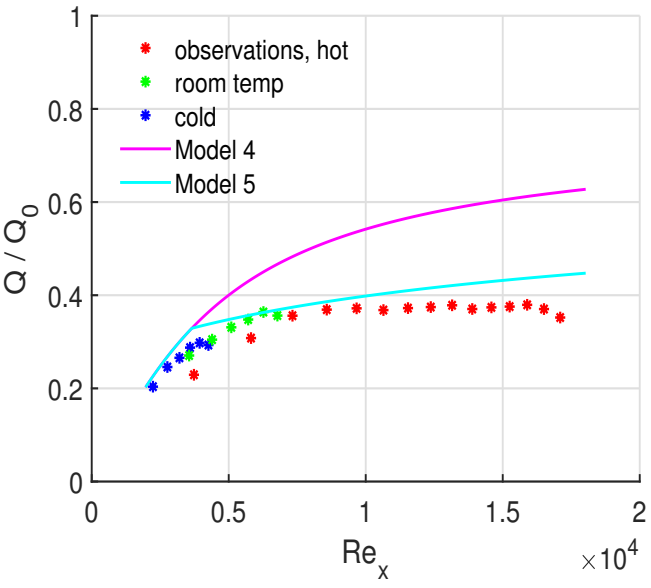

Figure 12: Red, green and blue points are the observed, nondimensional transport $Q\,/\,Q_0$ from the experiments of Fig. 5 shown here as a function of Re_x. These three experiments are at a common $L\,/\,d \;=\; 140$, but have different viscosity due to different temperature. The cyan line is the corresponding Model 4 prediction which overestimates the transport at larger Re_x. Notice the change in the nondimensional transport at very roughly $Re_x \;=\; 7000$, which corresponds to an internal Reynolds number, $Re \;=\; Re_x\,(Q\,/\,Q_0) \;\approx\; 2500$. This is interpreted to be a result of a transition from (somewhat) turbulent flow at larger Re_x to laminar flow at smaller Re_x.
A better prediction comes from Model 5, the magenta line, that implements an adjustment of the viscosity to account for turbulent flow.

not do is deal with actual, wet water running through a pipe. That is the central problem which we ought to solve some day, and we have not."[22] By 'solve', Feynman was contrasting the empirical treatment of turbulent flows (coming below) with the Poiseuille solution from first principles that solves laminar pipe flow. A great deal has been learned regarding the remarkably complex phenomena that make up a turbulent pipe flow,[23] which goes some way to explaining why we still do not have (and may never have) a concise, understandable solution for turbulent pipe flow based upon first principles. This strongly shapes the development of a model intended to account for turbulent flow effects.

While we do not have a first-principles solution for turbulent pipe flow, what we *do* have is a vast body of historical data and analyses. Many of these experimental studies came in response to the practical need to predict the pressure drop, δP, that will be required to drive a given fluid at a specified mean velocity, V_a, through a given pipe. Dimensional analysis of this problem is

- A VPlist for the pressure drop along a pipe: (50)

1. pressure drop expressed as a hydrostatic head, $g\,h \;\doteq\; [\,0\;\;2\;\;\text{-}2\,]$, the dependent variable,

[22] R. Feynman, 'Lectures in Physics Vol. II', 1964, Addison-Wesley.

[23] An excellent, comprehensive review of the research on turbulent transition is by Avila, M, D. Barkley and B. Hof, 2023, 'Transition to turbulence in pipe flow', Ann. Rev. Fluid Mech., 55, 575-602. https://doi.org/10.1146/annurev-fluid-120720-025957

2. mean velocity, $V_a \doteq [\,0 \quad 1 \quad -1\,]$, an independent variable,
3. diameter of the pipe, $d \doteq [\,0 \quad 1 \quad 0\,]$, a parameter,
4. kinematic viscosity of the water, $\nu \doteq [\,0 \quad 2 \quad -1\,]$, a parameter,
5. length of the pipe, $L \doteq [\,0 \quad 1 \quad 0\,]$, a parameter.

Three nondimensional variables are expected, and as one possibility,

$$\frac{g\,h}{V_a^2\,/\,2} \;=\; f(\frac{L}{d},\; Re), \quad \text{where} \quad Re \;=\; \frac{V_a\,d}{\nu}. \tag{51}$$

This is a complement to the problem of viscous pipe flow discussed in Sec. 6.1 insofar as V_a and pressure have switched places — here in (51), V_a is the known, independent variable, and pressure ($g\,h$) is the unknown, dependent variable. Thus the Reynolds number of (51) is the internal Reynolds number, Re, rather than the external Reynolds number Re_x used extensively in Sec. 6. Since pressure is the dependent variable, it has been kept to the first power, and so V_a is quadratic in this relation.

If the flow within the pipe is independent of distance downstream (fully developed) then the pressure drop should be directly proportional to the pipe length, L. If so, then the parameter L/d may be taken out of the argument of f and included as a multiplying factor. This gives a widely used, simplified form

$$\boxed{\frac{g\,h}{V_a^2\,/\,2} \;=\; \frac{L}{d}\,f(\,Re\,)} \tag{52}$$

The unknown function of (52) is denoted by f, which is traditional in this role, and called the friction factor or oftentimes the 'Darcy' friction factor. The function $f(Re)$ has been the object of hundreds of experimental programs, and the results distilled into a Moody diagram, a simplified example is Fig. 13.[24] There is no doubt about the practical value of the Moody diagram, but the physical interpretation of f itself does not go very deep. f is not a model of turbulence, but rather an empirical measure of flow resistance, larger f corresponding to greater resistance. f is also not a fluid property but rather a joint property of the fluid, the flow and the pipe, organized by the dimensional analysis that lead to Eq. (52).

One part of the Moody diagram is clear and even familiar. In the low Re laminar flow regime, the Poiseuille solution gives

$$f(Re)_{laminar} \;=\; \frac{64}{Re}, \tag{53}$$

the blue line at left of Fig. 13. The higher Re turbulent flow regime is different and more interesting. One classical representation of $f(Re)$ for turbulent flow in a smooth pipe is the red solid curve at

[24] Estimation of the wall stress in real pipes often has to account for the surface roughness of the pipe wall. If the height of the roughness elements is ϵ, then the roughness will appear in Eq. (51) as a nondimensional parameter $\epsilon\,/\,d$. Moody diagrams generally display $f(Re)$ with $\epsilon/d \;=\; constant$ on a near-blizzard of curves that sit above and are more or less parallel to the curve for smooth pipes, the solid red line of Fig. 13; larger roughness results in larger wall stress. The 'pipes' used in the present experiments were new and clean and presumed to be smooth, and so roughness is neglected here; thus the somewhat impoverished Moody diagram of Fig. 13.

lower right, an empirical correlation of experimental data analyzed by Blasius in the 1910s,

$$f(Re)_{turbulent} \;=\; \frac{0.316}{Re^{1/4}}. \tag{54}$$

In what follows it will be necessary to have a function $f(Re)$ defined over the full range of Re. The presumption here is that $f(Re)$ follows the Poiseuille curve (53) for small Re until intersection with the Blasius curve Eq. (54) at $Re \;=\; 1200$. It continues as the Blasius curve thereafter. There is no special treatment within the transition region.[25]

The data from the present experiments may be used to evaluate $f(Re)$ using Eq. (52), and gives an interesting result, Fig. 14. The distribution is consistent in part with the historical data insofar as many of the experimental data fall close to the historical curves. That is reassuring; our little table-top apparatus is not highly anomalous, and so the results and broad conclusions reached here should be representative of pipe flows generally. But there are also many estimates of f that are well away from the historical curves, all in the direction of larger f. These high estimates are not measurement artifacts, but likely due to any one of several physical processes that are not accounted by a classical friction factor: surface tension (for very short pipes), entrance effects (for short pipes) which violate the fully-developed flow restriction,[14] and hysteresis (turbulent to laminar transition).[20] Each of these phenomena would be expected to enhance the flow resistance for a given Re. Surface tension was treated briefly in Sec. 4, but the latter two phenomena are beyond the scope of this study.

7.3 Estimating an effective viscosity for use within a laminar flow framework

To make use of the essential information provided by the historical $f(Re)$, the laminar plus turbulent curves of Fig. 13, the tactic will be to map $f(Re)$ into a so-called effective viscosity, ν_e. The intention is that ν_e will account for turbulence-enhanced flow resistance within the framework of Model 4. The question is — for a given Re and a given pipe, what value of an effective viscosity, ν_e, will give a transport (or V_a) consistent with the $f(Re)$ of Eq. (54)? From (52) it appears that

$$Q_{turbulent} \;\propto\; \frac{1}{f_{turbulent}^{1/2}}$$

within the turbulent flow regime, and from the laminar (Poiseuille) solution it is clear that

$$Q_{laminar} \;\propto\; \frac{1}{f_{laminar}} \;\propto\; \frac{1}{\nu}$$

[25] There are a number of more complex formulae that serve to connect smoothly the laminar and turbulent flow branches within the transition region.[19] A single, continuous function $f(Re)$ is desirable, but the differences compared with the present, simplified two-piece version are found to be very small.

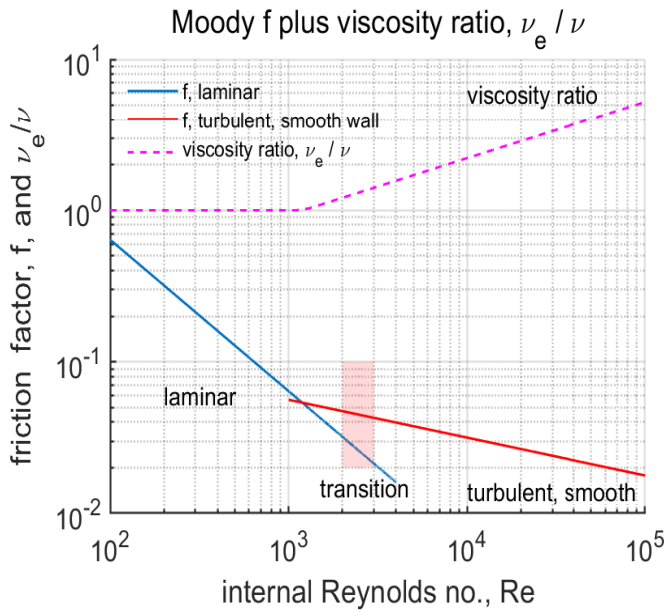

Figure 13: The friction factor, f, as a function of the internal Reynolds number, Re. The blue line at left comes from a laminar flow, i.e., Poiseuille's solution. The red curve at lower right is the Blasius fit to turbulent flow in a smooth pipe. The dashed, magenta line is the viscosity ratio computed from Eq. (56) and the constraint that ν_e/ν must be greater than 1. The light red shading indicates the transition region, the range of Reynolds numbers, very roughly 2000 - 3000, at which a laminar flow, if gently accelerated and not subjected to large amplitude perturbations, would likely show signs of instability and a transition to turbulent flow. In practice there is not a sharp boundary on the transition region, and neither is there a clear consensus on $f(Re)$ within this region.

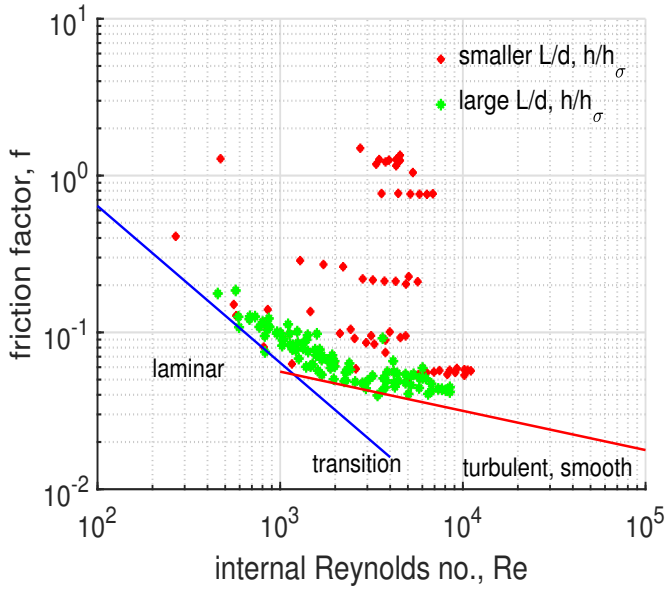

Figure 14: The friction factor, $f(Re)$, evaluated from the present experimental data, the red and green dots. The blue and red lines are as in the previous figure. The red dots represent data at smaller values of h/h_σ, likely affected by surface tension, and at smaller L/d that may be affected by entry length.[14] Neither of these phenomena is accounted by a friction factor, and it is not surprising that the red points are widely scattered. The distribution of the green points (all the rest of the data that are at larger h/h_σ and L/d) forms a cloud that is slightly above the historical curves and that more or less conforms with the change in slope of $f(Re)$ that is expected in the transition from laminar to turbulent flow at very roughly $Re \approx 2500$.

within the laminar flow regime. These will be consistent if

$$\frac{\nu_e}{\nu} \;=\; \sqrt{\frac{f_{turbulent}}{f_{laminar}}}, \tag{55}$$

the dashed magenta line labeled viscosity ratio in Fig. 13. A handy version of this comes from substitution of (53) and (54) into (55),

$$\frac{\nu_e}{\nu} \;=\; 7\times 10^{-2}\, Re^{3/8}, \quad \text{and,} \quad \nu_e/\nu \;\geq\; 1. \tag{56}$$

Eq. (56) may be evaluated for any $Re \;\geq\; 0$, but it is required that ν_e/ν must be $\geq\; 1$ on the basis that turbulence (or any other disturbance) will only make the effective viscosity larger than is the physical fluid viscosity, ν.

Implementation of an effective viscosity starts with a solution of Model 4. If that solution gives $Re \;\leq\; 1200$, then the flow is presumed to be laminar, $\nu_e \;=\; \nu$, and nothing more need be done. If instead $Re \geq 1200$, then the effective viscosity ν_e is evaluated from (56), and the solution recomputed with $\nu \;=\; \nu_e$. This first estimate of ν_e will be somewhat too large since the Model 4 estimate of Re will be too large. The solution is therefore iterated to arrive at an internally consistent solution in which the model-computed $f(Re)$ approximates the historical $f(Re)$. In all of this, the Reynolds numbers are evaluated with the actual fluid viscosity, ν, not the effective viscosity.[26]

It is important to understand that the so-called effective viscosity estimated by (56) is not a directly measurable, physical property of the fluid (the same thing was said earlier of f). Rather, ν_e is a modeling *device*, or in modern vernacular, a modeling *hack*, that allows the import of the historical laminar and turbulent flow relationship $f(Re)$ into the laminar flow framework of Model 4.

7.4 At last, Model 5

Model 5 is defined by the effective viscosity relation (56) and the algorithm to implement its use in a laminar flow framework. Over most of the parameter space of these experiments the effective viscosity is less than twice the actual fluid viscosity, the dashed magenta curve of Fig. 13. The consequences for the model-computed transport are significant at large Re_x, compare the Model 4' solution with the Model 5' solution in Fig. 10, but are not qualitative.

The mapping of $f(Re)$ to $\nu_e(Re)$, Eq. (56), should be regarded as a hypothesis, and not a fundamental law derived from first principles: it might work or it might not. Significantly, (56) is a *testable* hypothesis having consequences that we can readily check against observations. The changes

[26] A Matlab script that implements Model 5 is linked in Sec. 8.

in transport that result from an increased viscosity ($\nu_e > \nu$) are in a direction that reduces the positive bias of Model 4, an example is in Fig. 12. The Model 4 solution begins to depart noticeably from the observations at $Re_x \approx 7000$, while the Model 5 solution is closer to the observations, though still slightly high. When the solution of Model 5 (including surface tension) is compared directly to the entire dataset (no exclusions; the blue dots of Fig. 11), the coefficient of determination is found to be $R^2 = 0.95$ and hence Q_5 accounts for 95% of the variance in Q. The root mean square of the error, $Q - Q_5$, is 0.05 (nondimensional units), and the mean of the error is -0.008 (also nondimensional). The sign indicates that Q_5 is slightly higher than the data, on average, though the bias is much reduced compared to the bias of the Model 4 solution.

Model 5 appears to be empirically adequate over the rather small parameter space and given the limited precision of these experiments (small when compared to the immense range of possible pipe flows alluded to at the end of Sec. 2.1). The remaining differences between Model 5 and the present dataset give scant motivation or direction for further development and so we have come to the end of the development path previewed in Fig. 1.

7.5 Closing remarks

Recall that in Sec. 1.2 there was mention of two desirable traits in a model, clarity (or understandability) and adequacy to the phenomenon and data of interest. These are likely to be in tension: here it seems that Model 4 is understandable, and Model 5 is adequate to the data. Now it's time to add one more hurdle for the study overall, *viz.*, we shouldn't feel comfortable with a model, and should not be confident applying that model, unless we understand where in parameter space the model will fail. The present dataset is not extensive enough to reveal the limits of Model 5, but we can be certain that there are such boundaries, and they may not be too far away. The most likely point of failure is the relation (56) that maps $f(Re)$ to ν_e. And specifically, without understanding the physical basis for the Blasius correlation Eq. (54) and its application here, there is no sound basis for trusting Model 5 solutions outside the range of Re that was sampled here.

A more precise and robust experimental apparatus that allowed greater temporal and volumetric resolution would be highly desirable (see Rother, 2024, of footnote 1). One of the most useful improvements would be a taller tank that would permit larger outflow velocity and larger Reynolds numbers than were reachable with the very modest apparatus used here.

7.6 Problems

- The changes made by the implementation of an effective viscosity are evident in the shift of predicted transport closer to the one-to-one line in Fig. 11 (red dots, Model 4, to blue dots Model

5). The change is most evident in the middle range of transport values. Can you explain why this is the case?

- Up through Sec. 6 the essential nondimensional parameter was the external Reynolds number, Re_x. Then in Sec. 7 that role was taken by the much more often encountered (just plain) Reynolds number, Re, dubbed the internal Reynolds number in Sec. 6. Can you explain why the sudden changeover from Re_x to Re, aside from historical precedent?

- Fig. 6 was (probably) difficult to appreciate on first sight. What can you now understand of it?

  i) What parameter space is defined by the coordinate axes of this figure? What is the parameter space sampled by the observations? What part of the figure's parameter space was inaccessible to the experiments? (hint: think Venn diagram).
  ii) Where is there evidence of a surface tension effect? Why not in other data?
  iii) Where in this figure is the most obvious evidence of a viscous drag effect on a laminar flow?
  iv) Why does the (inferred) surface $F(L/d,\ Re_x)$ flatten out at large Re_x and large L/d?

- **Farewell, Explorer.**

Off to find new worlds.
With Earth's gift of fresh insight,
She will make her way.

With business finally finished (tank drained) and with a backpack full of new codes and diagrams, Planetary Explorer blasted off in search of new planets and adventures. Soon she discovered a new and somewhat barren planet, and most surprising, another tank-draining project. There were two obstacles not encountered on verdant Earth: no Matlab and no internet. Assuming that the local gravitational acceleration g can be measured independently, how might the diagrams of this appendix be used to predict the gravity-driven outflow rate on this new planet?

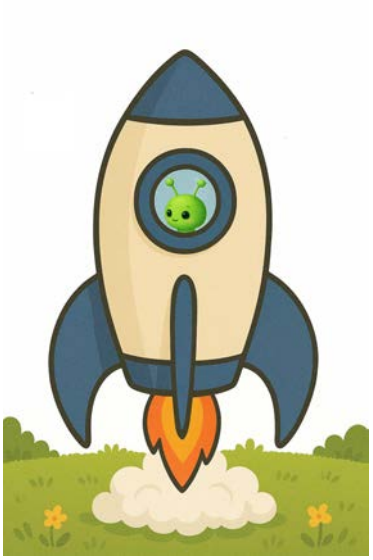

Planetary Explorer blasting off.
Image by the author using ChatGPT-5.

- Advanced exploration for Earthlings. At the outset of Sec. 6 a dimensional analysis was applied to pressure-driven, viscous, fully-developed pipe flow. Repeating the VPlist for convenience,

  Pressure-driven transport of a fully-developed, viscous pipe flow: (33r)

  volume transport, $Q \doteq$ [0 3 -1], the dependent variable,
  pressure gradient, $\partial P/\partial x \doteq$ [1 -2 -2], an independent variable,
  radius of the pipe, $r \doteq$ [0 1 0], a parameter,
  dynamic viscosity, $\mu \doteq$ [1 -1 -1], a parameter.

  This VPlist yields a basis set having just one nondimensional variable that must be a constant,

$$\frac{Q\,\mu}{r^4\ \partial P/\partial x} \ = \ constant. \tag{34r}$$

The result (34r) has the form of Poiseuille's linear, laminar solution, in which transport is directly proportional to the pressure gradient. In this Sec. 7 we have seen that the transport of a pipe flow may also depend upon the properties of the flow itself, whether laminar or turbulent. Where in (33r) is the possibility of turbulence? Or said a little differently, why is a linear, laminar flow guaranteed by this specific VPlist?

The VPlist (33r) included a small choice that had larger consequences than might be anticipated. The parameters pressure gradient and dynamic viscosity both included the dimension, mass. Fair enough, they usually do. But since the dependent variable was taken to be the volume transport, Q, which does not contain a mass dimension, then the viscosity and pressure gradient were bound to appear in the resulting basis set as their ratio, call it $\alpha \ = \ \mu\,(\partial P/\partial x)^{-1}$, and $\alpha \ \doteq \ [0\ 1\ 1]$. The VPlist (33r) had, in effect, only three independent dimensional variables, Q, r and α, and just two dimensions, length and time. This implies that there will be only one nondimensional variable, as there is in (34r), which is consistent with Poiseuille's solution for linear, laminar flow. In other words, there is no allowance in the basis set (34r) for a turbulent flow in which transport is not directly proportional to the pressure gradient.

Let's try an experiment: starting with the VPlist (33r), divide the dynamic viscosity by the fluid density to get the kinematic viscosity, and similarly for the pressure gradient to recast as an acceleration. We are not concerned in this study with the possibility of a variable fluid density, and so these choices should be acceptable, physically.

Pressure-driven transport of a fully-developed, viscous pipe flow, omitting mass:

volume transport, $Q \ \doteq \ [\,0 \ \ 3 \ \ -1\,]$, the dependent variable, (57)
pressure gradient acceleration, $(\partial P/\partial x)\,/\,\rho \ \doteq \ [\,0 \ \ 1 \ \ -2\ \,]$, an independent variable,
radius of the pipe, $r \ \doteq \ [\,0 \ \ 1 \ \ 0\,]$, a parameter,
kinematic viscosity, $\nu \ = \ \mu\,/\,\rho \ \doteq \ [\,0 \ \ 2 \ \ -1\,]$, a parameter.

There are four members in the revised VPlist, just as before, but now with only two dimensions, length and time. Compute the basis set of nondimensional variables and find two members,

$$\frac{Q}{d\,\nu} \ = \ F(\frac{d^3\,((\partial P/\partial x)\,/\,\rho)}{\nu^2}), \tag{58}$$

a nondimensional transport that is equal to an unknown function of a Reynolds-like number. This revised analysis can accommodate turbulent flow and laminar flow, and yet it has sprung from a reduced and seemingly simpler VPlist compared with (33r).

Below are some experiments that will help fill out this discussion. The repeated null space calculations implied here are best done with Matlab or Python codes linked in the next section.

i) Starting with the VPlist (33r), change the dependent variable to mass transport, $Q_m \ \doteq \ [\,1\ 0\ -1\,]$, but leave all else the same. This is the complement to the example worked above in the sense that all possible instances of mass are included in the VPlist. Compute the nondimensional basis set, and compare with Eq. (34r).

ii) Starting with the VPlist (33r), replace the dynamic viscosity with kinematic viscosity (as if dividing by a constant density) but leave all else as is. This will not go well to the extent that the nondimensional basis set will have to omit the pressure gradient, the motive power for the flow. What went wrong?

iii) There are several more variations on this mass in or mass out exercise, and it is revealing to approach them systematically. Start with the VPlist (33r), and set plausibility aside. Allow that the three variables Q, $\partial P \,/\, \partial x$, and μ can appear either with or without division by density; r continues along unbothered by all this. How many unique combinations (mass on, mass off for each relevant parameter) are there in this ensemble of VPlists? We have already considered two of them in i) and ii) above. How many of the ensemble VPlists will fail to give a sensible result, as in case ii) above? How many give the Poiseuille result, Eq. (34r)? How many give that $F = F(Re)$? Now allow physical reasoning back in. Which of the VPlists and solutions are the least arbitrary?

iv) Starting with the VPlist (33r), include the fluid density as a fifth member of the VPlist. Calculate the nondimensional variables of this augmented VPlist, and explain how your new result compares with Eq. (34r).

What's the moral of this short story / long problem? Because VPlists do not include much information to begin with, even a small and seemingly incidental omission or addition can have a qualitative effect on the result. As well, there is binary-like property to a VPlist; a parameter is either in or out, with no gradation for just a little effect of mass, for example. With that in mind, it is good practice to regard every new or unfamiliar VPlist as provisional, and to experiment with plausible variations to see if something unexpected may emerge.

8 Housekeeping

Attribution: The experiments, the models and codes, the text and the technical figures were made by the author. The Planetary Explorer images were created by the author using ChatGPT-5.

Acknowledgements: Administrative assistance was provided by the Dept. of Physical Oceanography, Woods Hole Oceanographic Institution.

Links to codes and data:

The calculation of a null space basis may be done with
Matlab: https://www2.whoi.edu/staff/jprice/wp-content/uploads/sites/199/2024/06/DanalysisA2.zip
Python: https://www2.whoi.edu/staff/jprice/wp-content/uploads/sites/199/2024/10/DA2Python.zip

The experimental data, the models and a Matlab script to exercise both are available at
https://www2.whoi.edu/staff/jprice/wp-content/uploads/sites/199/2025/12/DA-tank.zip
There are four files:

- Dstruct.mat, a Matlab structure that stores all of the experimental data.
- DAtank.xlsx, same as above but in an Excel table file.
- Model5.m, a Matlab function that evaluates Model 5, and with the appropriate settings, Model 4.
- Dplot.m, a Matlab script that loads Dstruct.mat and makes several plots of the data, including a 3-dimensional version of the present Fig. 6 along with model predictions.

Index

Resource: Topics in Fluid Dynamics

James F. Price